Inorg. Chem. **2007**, *46*, 5651–5664

Wirelike Dinuclear Ruthenium Complexes Connected by Bis(ethynyl)oligothiophene

Li-Bin Gao,[†] Jian Kan,[†] Yang Fan,[†] Li-Yi Zhang,[†] Sheng-Hua Liu,[‡] and Zhong-Ning Chen*[,†,§]

State Key Laboratory of Structural Chemistry, Fujian Institute of Research on the Structure of Matter, The Chinese Academy of Sciences, Fuzhou, Fujian 350002, China, Key Laboratory of Pesticide and Chemical Biology, College of Chemistry, Central China Normal University, Wuhan 430079, China, and State Key Laboratory of Organometallic Chemistry, Shanghai Institute of Organic Chemistry, The Chinese Academy of Sciences, Shanghai 200032, China

Received March 2, 2007

Preparation and characterization of a series of rodlike binuclear ruthenium polyynediyl complexes capped with redox-active organometallic fragments $[(bph)(PPh_3)_2Ru]^+$ (bph = *N*-(benzoyl)-*N*′-(picolinylidene)-hydrazine) or $[(Phtpy)(PPh_3)_2Ru]^{2+}$ (Phtpy = 4′-phenyl-2,2′:6′,2″-terpyridine) have been carried out. The length of the molecular rods is extended by successive insertion of 2,5-thiophene or 1,4-phenylene spacers in the bridging ligands. Oxidation of thiophene-containing $Ru_2^{II,II}$ complexes induces isolation of stable $Ru_2^{II,III}$ or $Ru_2^{III,III}$ species. Electrochemical and UV–vis–NIR spectral studies demonstrate that the polyynediyl bridges with 2,5-thiophene units are more favorable for metal–metal charge transfer compared with those containing the same number of 1,4-phenylene units. Successive increase of thiophene spacers in mixed-valence complexes $\{Ru^{II}\}–C{\equiv}C(C_4H_2S)_mC{\equiv}C–\{Ru^{III}\}$ (m = 1, 2, 3) induced a smooth transition from almost electronic delocalization (m = 1) to localization (m = 3). For binuclear ruthenium complexes with intramolecular electron transfer transmitted across nine Ru–C and C–C bonds, electronic conveying capability follows $\{Ru\}–C{\equiv}C(C{\equiv}C)_2C{\equiv}C–\{Ru\} > \{Ru\}–C{\equiv}C(C_4H_2S)C{\equiv}C–\{Ru\} > \{Ru\}–C{\equiv}C(C_6H_4)C{\equiv}C–\{Ru\} > \{Ru\}–C{\equiv}C(CH{=}CH)_2C{\equiv}C–\{Ru\}$. It is revealed that molecular wires capped with electron-rich $(bph)(PPh_3)_2Ru$ endgroups are much more favorable for electronic communication than the corresponding electron-deficient $(Phtpy)(PPh_3)_2Ru$-containing counterparts. The intermetallic electronic communication is fine-tuned by modification of both the bridging spacers and the ancillary ligands.

Introduction

Long-distance communications including electron or energy transfer between remote metal centers are the most fundamental aspects of information conveying in molecular electronics. The controlling and tuning of these communications are of experimental significance and especially practical.[1−6] Since the discovery of the Creutz−Taube ion $[(NH_3)_5Ru{-}pyrazine{-}Ru(NH_3)_5]^{5+}$,[7] it has been well documented that mixed-valence metal complexes bridged by conjugated organic ligands and capped with redox-active organometallic termini allow facile intramolecular electron transfer to occur along the molecular backbone.[8,9] Such linear organometallic systems with extended π-conjugation are attractive candidates for potential molecular wires, which might operate as connectors permitting electron flow to occur between different elements of nanoscale electronic devices by virtue of the possible charge delocalization along the conjugated molecular backbones. The current challenge consists not only in the synthesis of such rodlike molecules possessing two redox-active termini connected through a

* To whom correspondence should be addressed. E-mail: czn@fjirsm.ac.cn.
† Fujian Institute of Research on the Structure of Matter.
‡ Central China Normal University.
§ Shanghai Institute of Organic Chemistry.

(1) Swager, T. M. *Acc. Chem. Res*. **1996**, *31*, 201.
(2) Astruc, D. *Acc. Chem. Res*. **1997**, *30*, 383.
(3) Launay, J.-P. *Chem. Soc. Rev*. **2001**, *30*, 386.
(4) Robertson, N.; McGowan, C. A. *Chem. Soc. Rev*. **2003**, *32*, 96.
(5) Carroll, R. L.; Gorman, C. B. *Angew. Chem., Int. Ed*. **2002**, *41*, 4378.
(6) D'Alessandro, D. M.; Keene, F. R. *Chem. Rev*. **2006**, *106*, 2270.
(7) (a) Creutz, C.; Taube, H. *J. Am. Chem. Soc*. **1969**, *91*, 3988. (b) Creutz, C.; Taube, H. *J. Am. Chem. Soc*. **1973**, *95*, 1086.
(8) Demadis, K. D.; Hartshorn, C. M.; Meyer, T. J. *Chem. Rev*. **2001**, *101*, 2655.
(9) Nelsen, S. F. *Chem.—Eur. J*. **2000**, *6*, 581.

10.1021/ic700412m CCC: $37.00
Published on Web 05/19/2007

π-system but also in the evaluation of their electron conduction capability.[10] Electrochemical measurements and spectroscopic studies in the near-infrared region are commonly employed to evaluate the capability of electronic interaction between remote electro-active organometallic groups and to access a series of decisive information on the metal−metal charge-transfer process in the mixed-valence compounds with extended π-delocalization. Relevant studies in recent years have principally been focused on elucidating the role of redox-active organometallic groups, judiciously selecting the conjugated bridging ligands as electron mediators, and fine-tuning the long-range interactions between remote metal centers by modifying the electronic effect in the ancillary ligands.[10] In most cases, the mixed-valence complexes can be categorized according to the classification proposed by Robin and Day[11] and analyzed theoretically using the Hush model initially established by Hush[12] in 1967 and developed later by others.[8,9,13]

Among different approaches to construct the wirelike organometallic entities, compounds with unsaturated carbon chains spanning two metal-containing components have received particular attention due to their facile accessibility and remarkable efficiency for electronic delocalization.[10,14−19] These compounds have shown a promising potential for the development of nanoscopic molecular devices. Particular efforts have been taken to prepare and characterize polyynediyl arrays $\{M\}-(C\equiv C)_m-\{M\}$ ($m = 1, 2, 3$, etc.),[20−32] polyylenediyl complexes $\{M\}-(CH=CH)_m-\{M\}$,[33−35] and bimetallic molecular rods linked by π-conjugated carbon chains with both ethynyl and ethenyl.[36,37] Very recently, another family of complexes with the carbon chains containing both ethynyl and para-substituted phenylene have been described,[38,39] in which the π-conjugated molecular lengths are extended by successive insertion of 1,4-phenylene units, inducing a progressive transition from electronic delocalized class III

(10) Paul, F.; Lapinte, C. *Coord. Chem. Rev.* **1998**, *178−180*, 431.
(11) Robin, M. B.; Day, P. *Adv. Inorg. Chem. Radiochem.* **1967**, *10*, 247.
(12) (a) Allen, G. C.; Hush, N. S. *Prog. Inorg. Chem.* **1967**, *8*, 357. (b) Hush, N. S. *Prog. Inorg. Chem.* **1967**, *8*, 391.
(13) Brunschwig, B. S.; Creutz, C.; Sutin, N. *Chem. Soc. Rev.* **2002**, *31*, 168.
(14) Long, N. J.; Williams, C. K. *Angew. Chem., Int. Ed.* **2003**, *42*, 2586.
(15) Szafert, S.; Gladysz, J. A. *Chem. Rev.* **2003**, *103*, 4175.
(16) Ren, T. *Organometallics*. **2005**, *24*, 4854−4870.
(17) Bruce, M. I.; Low, P. J. *Adv. Organomet. Chem*. **2004**, *50*, 179.
(18) Touchard, D.; Dixneuf, P. H. *Coord. Chem. Rev.* **1998**, *178−180*, 409.
(19) Akita, M.; Sakurai, A.; Chung, M.-C.; Moro-oka, Y. *J. Organomet. Chem*. **2003**, *670*, 2.
(20) (a) de Montigny, F.; Argouarch, G.; Costuas, K.; Halet, J.-F.; Roisnel, T.; Toupet, L.; Lapinte, C. *Organometallics* **2005**, *24*, 4558. (b) Paul, F.; Meyer, W. E.; Toupet, L.; Jiao, H.; Gladysz, J. A.; Lapinte, C. *J. Am. Chem. Soc*. **2000**, *122*, 9405. (c) Narvor, N. L.; Toupet, L.; Lapinte, C. *J. Am. Chem. Soc*. **1995**, *117*, 7129. (d) Courmarcel, J.; Gland, G. L.; Toupet, L.; Paul, F.; Lapinte, C. *J. Organomet. Chem*. **2003**, *670*, 108. (e) Guillaume, V.; Mahias, V.; Mari, A.; Lapinte, C. *Organometallics* **2000**, *19*, 1422. (f) Coat, F.; Guillevic, M.-A.; Toupet, L.; Paul, F.; Lapinte, C. *Organometallics* **1997**, *16*, 5988. (g) Coat, F.; Lapinte, C. *Organometallics* **1996**, *15*, 477.
(21) (a) Dembinski, R.; Bartik, T.; Bartik, B.; Jaeger, M.; Gladysz, J. A. *J. Am. Chem. Soc*. **2000**, *122*, 810. (b) Brady, M.; Weng, W.; Zhou, Y.; Seyler, J. W.; Amoroso, A. J.; Arif, A. M.; Böhme, M.; Frenking, G.; Gladysz, J. A. *J. Am. Chem. Soc*. **1997**, *119*, 775. (c) Jiao, H.; Costuas, K.; Gladysz, J. A.; Halet, J.-F.; Guillemot, M.; Toupet, L.; Paul, F.; Lapinte, C. *J. Am. Chem. Soc*. **2003**, *125*, 9511. (d) Weng, W.; Bartik, T.; Brady, M.; Bartik, B.; Ramsden, J. A.; Arif, A. M.; Gladysz, J. A. *J. Am. Chem. Soc*. **1995**, *117*, 11922. (e) Horn, C. R.; Gladysz, J. A. *J. Eur. Inorg. Chem*. **2003**, 2211. (f) Horn, C. R.; Martin-Alvarez, J. M.; Gladysz, J. A. *Organometallics* **2002**, *21*, 5386.
(22) (a) Rigaut, S.; Olivier, C.; Costuas, K.; Choua, S.; Fadhel, O.; Massue, J.; Turek, P.; Saillard, J. Y.; Dixneuf, P. H.; Touchard, D. *J. Am. Chem. Soc*. **2006**, *128*, 5859. (b) Rigaut, S.; Massue, J.; Touchard, D.; Fillaut, J.-L.; Golhen, S.; Dixneuf, P. H. *Angew. Chem., Int. Ed*. **2002**, *41*, 4513. (c) Uno, M.; Dixneuf, P. H. *Angew. Chem., Int. Ed*. **1998**, *37*, 1714. (d) Rigaut, S.; Perruchon, J.; Pichon, L. L.; Touchard, D.; Dixneuf, P. H. *J. Organomet. Chem*. **2003**, *670*, 37. (e) Rigaut, S.; Pichon, L. L.; Daran, J.-C.; Touchard, D.; Dixneuf, P. H. *Chem. Commun*. **2001**, 1206. (f) Rigaut, S.; Touchard, D.; Dixneuf, P. H. *J. Organomet. Chem*. **2003**, *684*, 68.
(23) (a) Bruce, M. I.; Low, P. J.; Costuas, K.; Halet, J.-F.; Best, S. P.; Heath, G. A. *J. Am. Chem. Soc*. **2000**, *122*, 1949. (b) Bruce, M. I.; Hall, B. C.; Kelly, B. D.; Low, P. J.; Skelton, B. W.; White, A. H. *J. Chem. Soc., Dalton Trans*. **1999**, 3719. (c) Bruce, M. I.; Hinterding, P.; Tiekink, E. R. T.; Skelton, B. W.; White, A. H. *J. Organomet. Chem*. **1993**, *450*, 209. (d) Bruce, M. I.; Ellis, B. G.; Low, P. J.; Skelton, B. W.; White, A. H. *Organometallics* **2003**, *22*, 3184. (e) Bruce, M. I.; Costuas, K.; Davin, T.; Ellis, B. G.; Halet, J.-F.; Lapinte, C.; Low, P. J.; Smith, M. E.; Skelton, B. W.; Toupet, L.; White, A. H. *Organometallics* **2005**, *24*.
(24) (a) Hu, Q. Y.; Lu, W. X.; Tang, H. D.; Sung, H. H. Y.; Wen, T. B.; Williams, I. D.; Wong, G. K. L.; Lin, Z.; Jia, G. *Organometallics* **2005**, *24*, 3966. (b) Xia, H.; Wen, T. B.; Hu, Q. Y.; Wang, X.; Chen, X.; Shek, L. Y.; William, I. D.; Wong, K. S.; Wong, G. K. L.; Jia, G. *Organometallics* **2005**, *24*, 562.
(25) (a) Antonova, A. B.; Bruce, M. I.; Ellis, B. G.; Gaudio, M.; Humphrey, P. A.; Jevric, M.; Melino, G.; Nicholson, B. K.; Perkins, G. J.; Skelton, B. W.; Stapleton, B.; White, A. H.; Zaitseva, N. N. *Chem. Commun*. **2004**, 960. (b) Bruce, M. I.; Ellis, B. G.; Gaudio, M.; Lapinte, C.; Melino, G.; Paul, F.; Skelton, B. W.; Smith, M. E.; Toupet, L.; White, A. H. *J. Chem. Soc., Dalton. Trans*. **2004**, 1601.
(26) (a) Kheradmandan, S.; Heinze, K.; Schmalle, H. W.; Berke, H. *Angew. Chem., Int. Ed*. **1999**, *38*, 2270. (b) Fernández, F. J.; Venkatesan, K.; Blacque, O.; Alfonso, M.; Schmalle, H. W.; Berke, H. *Chem.—Eur. J*. **2003**, *9*, 6192. (c) Fernández, F. J.; Blacque, O.; Alfonso, M.; Berke, H. *Chem. Commun*. **2001**, 1266. (d) Kheradmandan, S.; Fox, T.; Schmalle, H. W.; Venkatesan, K.; Berke, H. *J. Eur. Inorg. Chem*. **2004**, 3544.
(27) Gao, L.-B.; Zhang, L.-Y.; Shi, L.-X.; Chen, Z.-N. *Organometallics* **2005**, *24*, 1678.
(28) (a) Akita, M.; Tanaka, Y.; Naitoh, C.; Ozawa, T.; Hayashi, N.; Takeshita, M.; Inagaki, A.; Chung, M.-C. *Organometallics* **2006**. (b) Sakurai, A.; Akita, M.; Moro-oka, Y. *Organometallics* **1999**, *18*, 3241. (c) Akita, M.; Chung, M.-C.; Sakurai, A.; Sugimoto, S.; Terada, M.; Tanaka, M.; Moro-oka, Y. *Organometallics* **1997**, *16*, 4882.
(29) (a) Qi, H.; Gupta, A.; Noll, B. C.; Snider, G. L.; Lu, Y.; Lent, C.; Fehlner, T. P. *J. Am. Chem. Soc*. **2005**, *127*, 15218. (b) Stang, P. J.; Tykwinski, R. *J. Am. Chem. Soc*. **1992**, *114*, 4411. (c) Gil-Rubio, J.; Laubender, M.; Werner, H. *Organometallics* **2000**, *19*, 1365. (d) Gil-Rubio, J.; Laubender, M.; Werner, H. *Organometallics* **1998**, *17*, 1202. (e) Gevert, O.; Wolf, J.; Werner, H. *Organometallics* **1996**, *15*, 2806. (f) Field, L. D.; Turnbull, A. J.; Turner, P. *J. Am. Chem. Soc*. **2002**, *124*, 3692.
(30) (a) Xu, G.-L.; Zou, G.; Ni, Y.-H.; DeRosa, M. C.; Crutchley, R. J.; Ren, T. *J. Am. Chem. Soc*. **2003**, *125*, 10057. (b) Xu, G.-L.; DeRosa, M. C.; Crutchley, R. J.; Ren, T. *J. Am. Chem. Soc*. **2004**, *126*, 3728. (c) Xu, G.-L.; Crutchley, R. J.; DeRosa, M. C.; Pan, Q.-J.; Zhang, H.-X.; Wang, X.; Ren, T. *J. Am. Chem. Soc*. **2005**, *127*, 13354−13363.
(31) Wong, K.-T.; Lehn, J.-M.; Peng, S.-M.; Lee, G.-H. *Chem. Commun*. **2000**, 2259.
(32) Bear, J. L.; Han, B.; Wu, Z.; Van Caemelbecke, E.; Kadish, K. M. *Inorg. Chem*. **2001**, *40*, 2275.
(33) (a) Chung, M. C.; Gu, X.; Etzenhouser, B. A.; Spuches, A. M.; Rye, P. T.; Seetharaman, S. K.; Rose, D. J.; Zubieta, J.; Sponsler, M. B. *Organometallics* **2003**, *22*, 3485. (b) Etzenhouser, B. A.; Cavanaugh, M. D.; Spurgeon, H. N.; Sponsler, M. B. *J. Am. Chem. Soc*. **1994**, *116*, 2221. (c) Etzenhouser, B. A.; Chen, Q.; Sponsler, M. B. *Organometallics* **1994**, *13*, 4176. (d) Sponsler, M. B. *Organometallics* **1994**, *13*, 1920.
(34) (a) Liu, S. H.; Chen, Y.; Wan, K. L.; Wen, T. B.; Zhou, Z.; Lo, M. F.; Williams, I. D.; Jai, G. *Organometallics* **2002**, *21*, 4984. (b) Liu, S. H.; Xia, H.; Wen, T. B.; Zhou, Z. Y.; Jia, G. *Organometallics* **2003**, *22*, 737.
(35) (a) Maurer, J.; Winter, R. F.; Sarkar, B.; Fiedler, J.; Záliš, S. *Chem. Commun*. **2004**, 1900. (b) Maurer, J.; Sarkar, B.; Schwederski, B.; Kaim, W.; Winter, R. F.; Záliš, S. *Organometallics* **2006**, *25*, 3701. (c) Maurer, J.; Rainer, F.; Winter, R. F.; Sarkar, B.; Záliš, S. *J. Solid State Electrochem*. **2005**, *9*, 738.

mixed-valence behavior to weakly coupled class II mixed-valence systems.

Although the 1,4-diethynylbenzene $-C\equiv CC_6H_4C\equiv C-$ unit has been extensively used as a π-spacer in organic or organometallic oligomers and polymers,[38−40] increasing attention is currently diverted to molecular materials based on oligothiophene because of their remarkable capability for electron conduction and charge mobility.[41−45] Evidence indicates that thiophene-containing bridges provided a more effective conjugated connection between the metal donor and acceptor moieties than other aromatic linkers such as phenylene.[41] It is anticipated that α-coupled oligothiophene-functionalized diethynyls $C\equiv C(C_4H_2S)_mC\equiv C$ (m = 1, 2, 3) would be excellent candidates for metal−metal charge transfer and electronic transportation along the molecular backbones. By this consideration, a systematic study on a series of rodlike binuclear ruthenium polyynediyl complexes capped with redox-active organometallic units $[(bph)(PPh_3)_2Ru]^+$ (bph = *N*-(benzoyl)-*N*′-(picolinylidene)-hydrazine) or $[(Phtpy)(PPh_3)_2Ru]^{2+}$ (Phtpy = 4′-phenyl-2,2′:6′,2″-terpyridine) and connected by $C\equiv C(C_4H_2S)_mC\equiv C$ (m = 1, 2, 3) has been carried out, in which the molecular length is extended by successive introduction of thiophene spacers in the carbon-rich chains. Chemical oxidation of the $Ru_2^{II,II}$ complexes by addition of 1 or 2 equiv of ferrocenium hexafluorophosphate induced isolation of stable $Ru_2^{II,III}$ or $Ru_2^{III,III}$ species in the solid state. For the purpose of comparison, the corresponding counterparts with thiophene spacers replaced by 1,3-butadiynyl, 1,3-butadienyl, or 1,4-phenylene units are also described herein together with the corresponding complexes containing 2,5-bis(1,3-butadiynyl)-thiophene ($C\equiv CC\equiv C(C_4H_2S)C\equiv CC\equiv C$) or 1,4-bis(1,3-butadiynyl)benzene ($C\equiv CC\equiv C(C_6H_4)C\equiv CC\equiv C$) as a bridging ligand. We reported herein the preparation and characterization together with electrochemical and UV−vis−NIR spectroscopic investigations of this series of binuclear ruthenium molecular rods to systematically evaluate their capability for intramolecular electron transfer.

Results and Discussion

Syntheses and Characterization. The molecular drawings of $[(bph)(PPh_3)_2Ru]^+$-containing complexes are depicted in Scheme 1 and 2 with variations of the substituents in the auxiliary Schiff bases. A series of $[(Phtpy)(PPh_3)_2Ru]^{2+}$-containing binuclear ruthenium complexes **9**−**17** (Scheme 3) are prepared so as to compare with $[(bph)(PPh_3)_2Ru]^+$-containing counterparts. In order to examine the electronic mediating capability of 2,5-bis(1,3-butadiynyl)thiophene and 1,4-bis(1,3-butadiynyl)benzene, (Phtpy)$(PPh_3)_2$Ru-capped dinuclear complexes **12** and **13** are also synthesized. The corresponding (bph)$(PPh_3)_2$Ru-containing counterparts, however, were inaccessible although many efforts have been taken.

Binuclear ruthenium polyynediyl complexes are all prepared by reaction of (bph)$(PPh_3)_2$RuCl or $[(Phtpy)(PPh_3)_2Ru(acetone)](ClO_4)_2$ with $Me_3Si-C\equiv C-R-C\equiv C-SiMe_3$ via fluoride-catalyzed desilylation in the presence of potassium fluoride in refluxed methanol.[23,27,37] Purification of the products by alumina column chromatography give $Ru_2^{II,II}$ products in reasonable yields except for **1**, in which the $Ru_2^{II,III}$ complex $[\mathbf{1}]^+$ with mixed-valence is also isolated during chromatographic separation. As electron-rich character in the endgroup (bph)$(PPh_3)_2$Ru affords a considerably low redox potential, $Ru_2^{II,III}$ and $Ru_2^{III,III}$ species with thiophene spacers are accessible by stepwise oxidation of neutral $Ru_2^{II,II}$ complexes. Thus, controlled oxidation of thiophene-containing compounds **1**−**3** by addition of 1 and 2 equiv of ferrocenium hexafluorophosphate induces isolation of stable solid species $[\mathbf{1a}]^+-[\mathbf{3a}]^+$ ($Ru_2^{II,III}$) and $[\mathbf{1b}]^{2+}-[\mathbf{3b}]^{2+}$ ($Ru_2^{III,III}$), respectively.

The compounds are all characterized by microanalysis, ESI-MS spectrometry, and ^1H and ^{31}P NMR spectroscopies. Microanalytical data coincide well with the calculated values. For $[(bph)(PPh_3)_2Ru]^+$-containing compounds **1**−**8**, positive ion ESI-MS reveals that molecular ion fragments $[M]^+$, $[M - PF_6]^+$, and $[M - (PF_6)_2]^{2+}$ occur as the base peaks or principal peaks with high abundance for the neutral $Ru_2^{II,II}$, monocationic $Ru_2^{II,III}$, and dicationic $Ru_2^{III,III}$ species, respectively. For $[(Phtpy)(PPh_3)_2Ru]^{2+}$-containing complexes **9**−**17**, molecular ion peaks $[M - (ClO_4)_2]^{2+}$ are observed in high

(36) (a) Shi, Y.; Yee, G. T.; Wang, G.; Ren, T. *J. Am. Chem. Soc*. **2004**, *126*, 10552. (b) Xia, H. P.; Ng, W. S.; Ye, J. S.; Li, X. Y.; Wong, W. T.; Lin, Z.; Yang, C.; Jia, G. *Organometallics* **1999**, *18*, 4552. (c) Xia, H. P.; Wu, W. F.; Ng, W. S.; Williams, I. D.; Jia, G. *Organometallics* **1997**, *16*, 2940.

(37) Gao, L.-B.; Liu, S.-H.; Zhang, L.-Y.; Shi, L.-X.; Chen, Z.-N. *Organometallics* **2006**, *25*, 506.

(38) (a) Ghazala, S. I.; Paul, F.; Toupet, L.; Roisnel, T.; Hapiot, P.; Lapinte, C. *J. Am. Chem. Soc*. **200**6, *128*, 2463. (b) Klein, A.; Lavastre, O.; Fiedler, J. *Organometallics* **2006**, *25*, 635. (c) Medei, L.; Orian, L.; Semeikin, O. V.; Peterleitner, M. G.; Ustynyuk, N. A.; Santi, S.; Durante, C.; Ricci, A.; Sterzo, C. L. *Eur. J. Inorg. Chem*. **2006**, 2582.

(39) (a) Colbert, M. C. B.; Lewis, J.; Long, N. J.; Raithby, P. R.; Younus, M.; White, A. J. P.; Williams, D. J.; Payne, N. N.; Yellowlees, L.; Beljonne, D.; Chawdhury, N.; Friend, R. H. *Organometallics* **1998**, *17*, 3034. (b) Long, N. J.; Martin, A. J.; Biani, F. F.; Zanello, P. *J. Chem. Soc., Dalton Trans*. **1998**, 2017.

(40) (a) Lavastre, O.; Plass, J.; Bachmann, P.; Guesmi, S.; Moinet, C.; Dixneuf, P. H. *Organometallics* **1997**, *16*, 184. (b) Narvor, N. L.; Lapinte, C. *Organometallics* **1995**, *14*, 634. (c) Weyland, T.; Lapinte, C.; Frapper, G.; Calhorda, M. J.; Halet, J.-F.; Toupet, L. *Organometallics* **1997**, *16*, 2024. (d) Weyland, T.; Costuas, K.; Mari, A.; Halet, J.-F.; Lapinte, C. *Organometallics* **1998**, *17*, 5569. (e) Weyland, T.; Costuas, K.; Toupet, L.; Halet, J.-F.; Lapinte, C. *Organometallics* **2000**, *19*, 4228.

(41) Stott, T. L.; Wolf, M. O. *Coord. Chem. Rev*. **2003**, *246*, 89.

(42) (a) Zhu, Y.; Wolf, M. O. *J. Am. Chem. Soc*. **2000**, *122*, 10121. (b) Zhu, Y.; Millet, D. B.; Wolf, M. O.; Rettig, S. J. *Organometallics* **1999**, *18*, 1930. (c) Clot, O.; Wolf, M. O.; Patrick, B. O. *J. Am. Chem. Soc*. **2000**, *122*, 10456. (d) Moorlag, C.; Wolf, M. O.; Bohne, C.; Patrick, B. O. *J. Am. Chem. Soc*. **2006**, *127*, 6382. (e) Bayly, S. R.; Humphrey, E. R.; de Chair, H.; Paredes, C. G.; Bell, Z. R.; Jeffery, J. C.; McCleverty, J. A.; Ward, M. D.; Totti, F.; Gatteschi, D.; Courric, S.; Steele, B. R.; Screttas, C. G. *J. Chem. Soc., Dalton Trans*. **2001**, 1401.

(43) (a) Stang, S. L.; Paul, F.; Lapinte, C. *Organometallics* **2000**, *19*, 1035. (b) Roué, S.; Lapinte, C. *J. Organomet. Chem*. **2005**, *690*, 594.

(44) (a) Lewis, J.; Long, N. J.; Raithby, P. R.; Shields, G. P.; Wong, W.-Y.; Younus, M. *J. Chem. Soc., Dalton Trans*. **1997**, 4283. (b) Wong, W.-Y.; Choi, K.-H.; Lu, G.-L. *Organometallics* **2002**, *21*, 4475. (c) Li, P.; Ahrens, B.; Choi, K.-H.; Khan, M. S.; Raithby, P. R.; Wilson, P. J.; Wong, W.-Y. *J. Chem. Soc., Dalton Trans*. **2002**, 405. (d) Li, P.; Ahrens, B.; Feeder, N.; Raithby, P. R.; Teat, S. J.; Khan, M. S. *J. Chem. Soc., Dalton Trans*. **2005**, 874. (e) Wong, W.-Y.; Lu, G.-L.; Ng, K.-F.; Choi, K.-H.; Lin. Z. *J. Chem. Soc., Dalton Trans*. **2001**, 3250. (f) Chawdhury, N.; Long, N. J.; Mahon, M. F.; Ooi. L.-l.; Raithby, P. R.; Rooke, S.; White, A. J. P.; Williams, D. J.; Younus, M. *J. Organomet. Chem*. **2004**, *689*, 840.

(45) Justin Thomas, K. R.; Lin, J. T.; Wen, Y. S. *Organometallics* **2000**, *19*, 1008.

Scheme 1

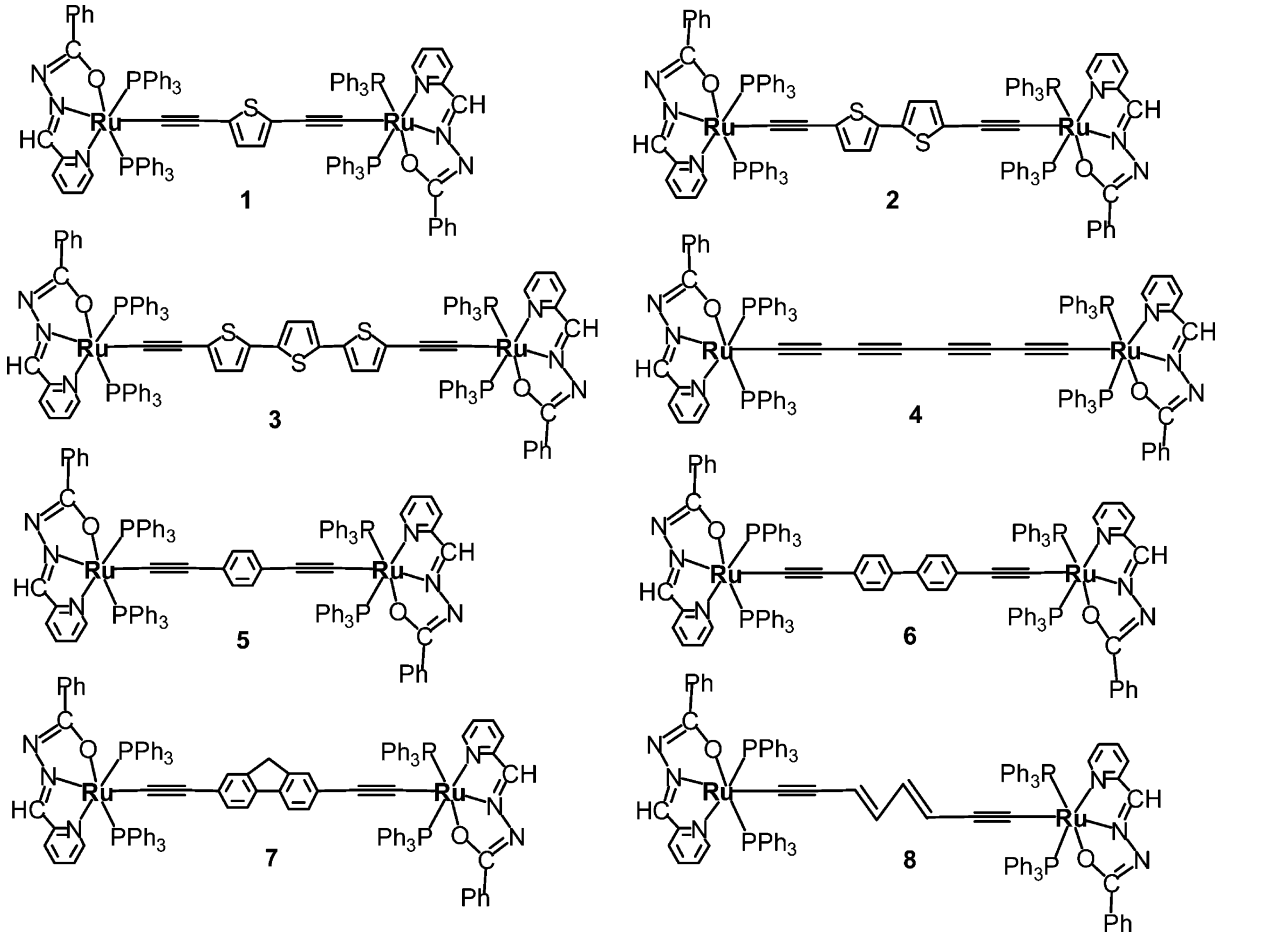

Scheme 2

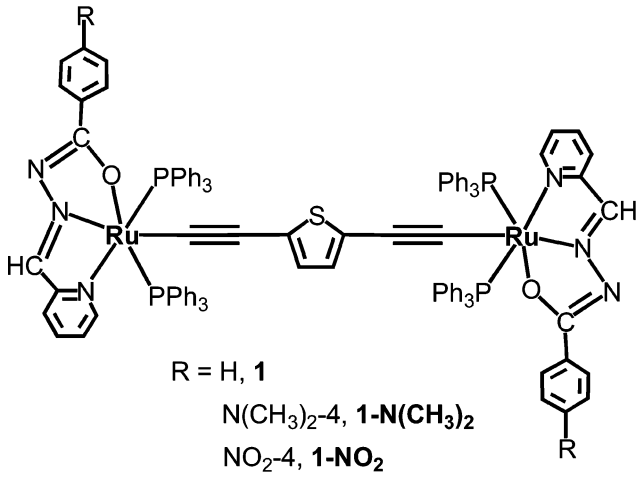

abundance. The ^{31}P NMR spectra show one singlet for PPh_3 donors in all of the complexes, indicating the equivalence of P donors in a wirelike diruthenium complex on the NMR time scale. It is intriguing that with stepwise oxidation of the $Ru_2^{II,II}$ centers, the P signals show a gradual shift to high-field, in which chemical shifts of the P donors in a series of species with different valences follow $Ru_2^{II,II}$ > $Ru_2^{II,III}$ > $Ru_2^{III,III}$.[27]

Crystal Structure. The structures of **2**·$2H_2O$·$2C_2H_4Cl_2$, **4**·Et_2O, and **6** were determined by X-ray crystallography. Selected bonding lengths and angles are presented in Tables S1, S2, and S3 (Supporting Information) for **2**, **4**, and **6**, respectively. ORTEP drawings of **2**, **4**, and **6** are depicted in Figure 1.

The rodlike binuclear ruthenium array **2**, **4**, or **6** consists of two (bph)$(PPh_3)_2$Ru endgroups linked by a diacetylide-containing carbon chain through Ru−C σ-bonding. The Ru^{II} centers are six-coordinated to exhibit an elongated octahedral geometry built by CN_2OP_2 donors, in which the two axially bonded PPh_3 are trans-oriented. The related bonding parameters including Ru−N_{py}, Ru−N_{imine}, Ru−O_{amide}, and Ru−P distances together with the trans and cis angles around the Ru^{II} octahedron are comparable to those found in the precursor complex (bph)$(PPh_3)_2$RuCl.[46] The bph serves as a tridentate ligand to afford two five-membered chelating rings. The N−N, N−C, and C−O distances in the ═N−N═C(O)− fragment imply the presence of an enolate form for the amide group. The Ru−C lengths (2.023(2)−2.037(4) Å) and Ru−C≡C angles (171.0(2)−176.7(4)°) are in the normal ranges as those found in other Ru^{II} acetylide complexes.[22,23,27,37]

Complex **2** is centrosymmetric with the inversion center at the midpoint of the C6−C6A bond. The equatorial plane of the Ru^{II} coordinating octahedron forms a dihedral angle of 25.7° with the thienyl plane in the bridging ligand. The two symmetry-related thienyl rings in the bridging ligand C≡C$(C_4H_2S)_2$−C≡C are coplanar and antioriented. The

(46) Raveendran, R.; Pal, S. *Polyhedron* **2003**, *24*, 57.

Scheme 3

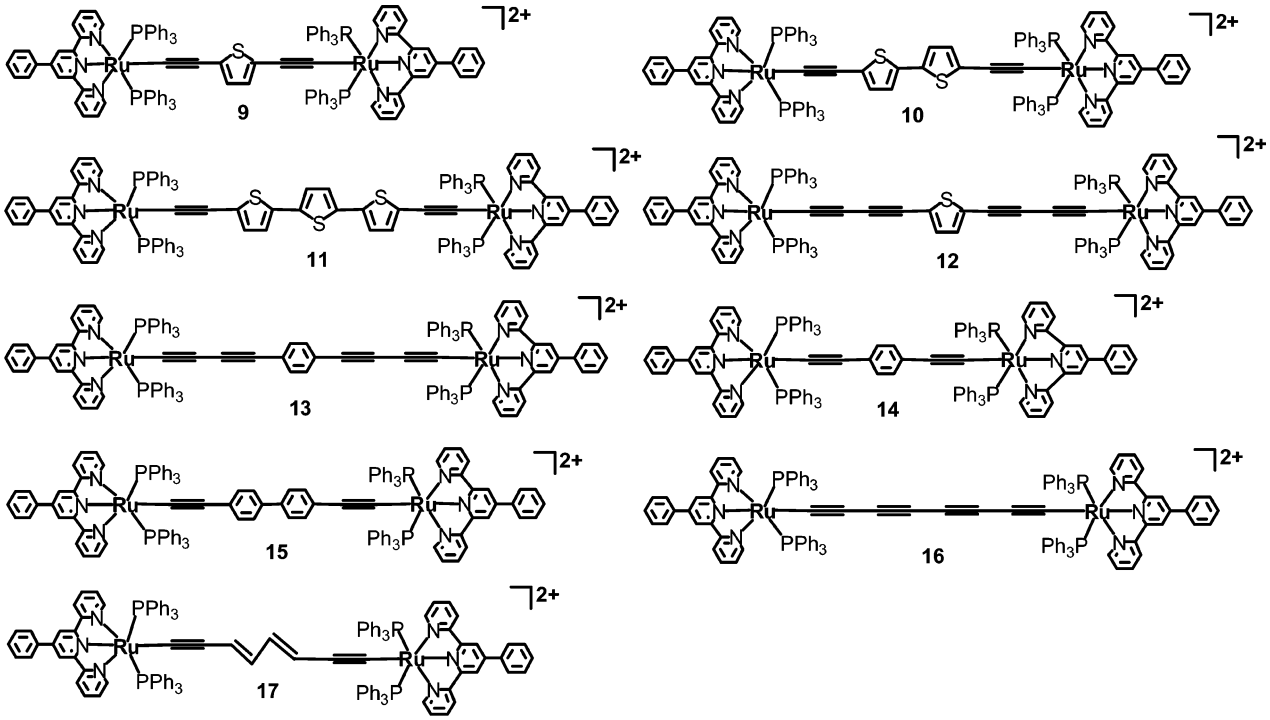

Ru1···Ru1A separation across the bridging 5,5′-diethynyl-2,2′-bithiophene is 15.3 Å, similar to the Pt···Pt distance in the binuclear Pt^{II} complex *trans*-[{$(Et_3P)_2PhPt$}$_2$($C{\equiv}C(C_4H_2S)_2{-}C{\equiv}C$)].[44a] The C≡C length (1.201(8) Å), however, is slightly shorter than that (1.25(3) Å) in the binuclear Pt^{II} complex,[44a] ascribed probably to the better back-donation capability for the Ru^{II} centers in **2**.

The C_8-bridged binuclear complex **4** has no symmetry in the molecule. The dihedral angle between the least-square plane defined by the bph ligand in one end and that in the other end is 84.6°, suggesting that the equatorial planes of the Ru1 and Ru2 centers are nearly perpendicular to each other. The Ru1···Ru2 distance through a bridging C_8 chain is 12.765 Å which is slightly shorter than the sum of the bond distances (13.027 Å) in the Ru−C≡C−C≡C−C≡C−C≡C−Ru array, indicating that the rod is somewhat distorted. The Ru−C≡C and C≡C−C angles (169.9(3)−179.3(3)°), however, deviate more obviously from 180° than those (<5° from 180° in general) reported in other C_8-bridged ruthenium complexes reported by Ren et al.,[30a] inducing a more distinct deviation from linearity in the Ru−C≡C−C≡C−C≡C−C≡C−Ru array. As depicted in Figure 1b, the accumulation of the bend results in a dramatic concave carbon chain.[20g,47b] Similar curvature has been observed in some Pt-capped compounds with the bridging C_8 chain described by Gladysz et al.[48]

Complex **6** is also centrosymmetric with the inversion center at the midpoint of the C6−C6A bond. The least-square plane defined by the bph ligand forms a dihedral angle of 73.5° with the biphenyl plane in the 4,4′-diethynylbiphenyl ligand. The two symmetry-related phenyl rings in the 4,4′-biphenyl spacer are coplanar, indicating that the steric interaction between the 3,5- and the 3′,5′-hydrogen atoms of the 4,4′-biphenyl spacer is insignificant.[49] The Ru1···Ru1A distance through the bridging 4,4′-diethynylbiphenyl is 16.5 Å, comparable to the intermetallic separations reported in the binuclear Fe^{II} and Mn^{II} complexes linked by 4,4′-diethynylbiphenyl.[26d,38a,c]

Redox Properties. The redox properties of compounds **1**−**17** in 0.1 M (Bu^n_4N)(PF_6) dichloromethane solutions have been investigated by cyclic and differential pulse voltammetry. The electrochemical data are presented in Table 1, and the plots of the cyclic voltammogram (CV) and the differential pulse voltammogram (DPV) for compounds **1**−**3** are depicted in Figure 2. The precursor compound (bph)-(PPh_3)$_2$RuCl displays a reversible metal-centered oxidation wave at $E_{1/2}$ = 0.060 V (against Fc^+/Fc) together with an irreversible bph ligand-based reduction wave at −1.30 V.[46] The ligand-centered reduction process is also detected in the binuclear ruthenium complexes **1**−**17** with the potential range from −1.30 to −1.91 V as listed in Table 1.

The CV and DPV in binuclear ruthenium complexes **1**−**17** are featured by two successive reversible redox waves A and B (Table 1) in the potential region from −0.70 to 0.37 V, originating most likely from successive oxidation of $Ru_2^{II,II}$ to $Ru_2^{II,III}$ and then $Ru_2^{II,III}$ to $Ru_2^{III,III}$, respectively. It has been demonstrated that the wave separation or potential difference ($\Delta E_{1/2} = E_{1/2}(B) - E_{1/2}(A)$) between waves A and B is a critical measure to evaluate electronic delocalization

(47) (a) Bruce, M. I.; Halet, J.-F.; Guennic, B. L.; Skelton, B. W.; Smith, M. E.; White, A. H. *Inorg. Chim. Acta* **2003**, *350*, 175. (b) Coat, F.; Paul, F.; Lapinte, C.; Toupet, L.; Costuas, K.; Halet, J.-F. *J. Organomet. Chem.* **2003**, *683*, 368.

(48) Stahl, J.; Bohling, J. C.; Bauer, E. B.; Peters, T. B.; Mohr, W.; Martín-Alvarez, J. M.; Hampel, F.; Gladysz, J. A. *Angew. Chem., Int. Ed.* **2002**, *41*, 1871.

(49) (a) Chao, H.-Y.; Lu, W.; Li, Y.; Chan, M. C. W.; Che, C.-M.; Cheung, K.-K.; Zhu, N. *J. Am. Chem. Soc.* **2002**, *124*, 14696. (b) Liu, L.; Poon, S.-Y.; Wong, W.-Y. *J. Organomet. Chem.* **2005**, *690*, 5036.

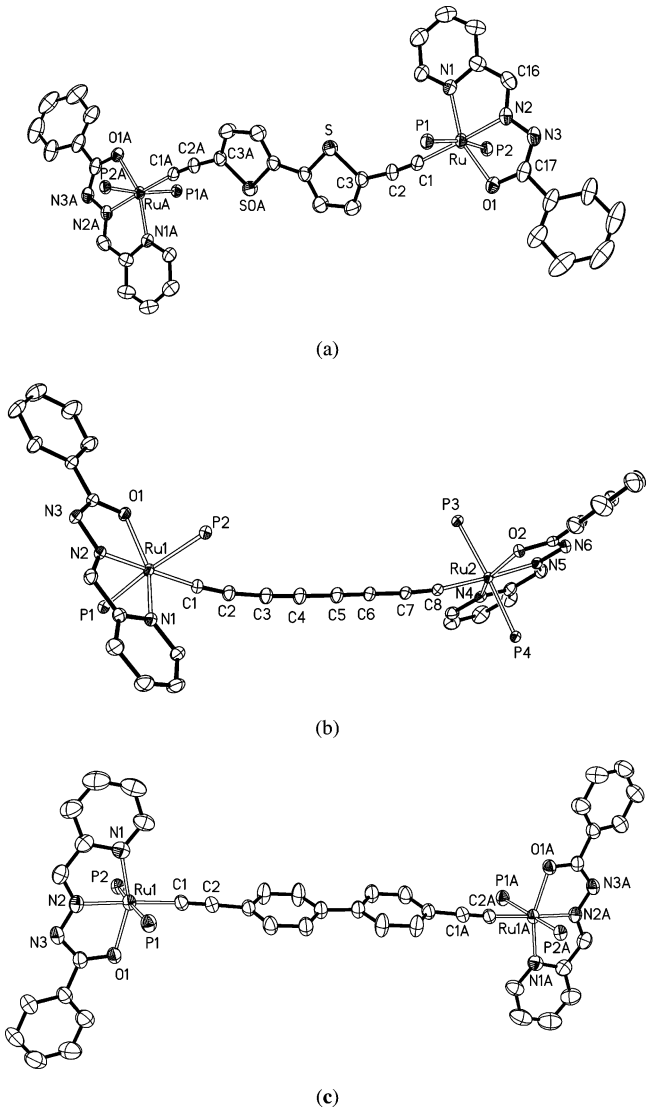

Figure 1. ORTEP drawing of (a) **2**, (b) **4**, and (c) **6** with atom labeling scheme showing 30% thermal ellipsoids. Phenyl rings on the phosphorus atoms are omitted for clarity.

along the molecular backbones in $Ru_2^{II,III}$ mixed-valence species.[10] Moreover, the $\Delta E_{1/2}$ values is correlated to the comproportionation constant K_c in the reaction $Ru_2^{II,II} + Ru_2^{III,III} \rightleftharpoons Ru_2^{II,III}$ and to the thermodynamic stability of the $Ru_2^{II,III}$ mixed-valence species.[50]

In complexes **1**−**3** with diethynyloligothiophene C≡C$(C_4H_2S)_m$C≡C (m = 1, 2, 3) as a connector, the $\Delta E_{1/2}$ values are 0.345, 0.170, and 0.100 V with the corresponding K_c being 6.80×10^5, 748, and 49, respectively. A considerably large K_c in **1** is indicative of a strong electronic communication transmitted through the 2,5-diethynylthiophene bridge. A successive insertion of two and three thiophene units into the diynediyl in **2** and **3**, respectively, induces a progressive reduction of the $\Delta E_{1/2}$ values. Even so, a weak but appreciable electronic interaction is still operative along the molecular backbone in **3** with the Ru···Ru separation close to 19.2 Å. In addition, another irreversible or quasireversible redox wave with higher potential is observed at 0.70, 0.59, and 0.44 V for **1**, **2**, and **3**, respectively, ascribed tentatively to oxidation of the thiophene ligands.[42,43] It is noteworthy that the potential and reversibility

Table 1. Electrochemical Data for Compounds **1**−**17**[a]

compound	$E_{1/2}$(A)	$E_{1/2}$(B)	$\Delta E_{1/2}$[b]	K_c[c]	$E_{thienyl}$[d]	E_{pc}[e]
(bph)$(PPh_3)_2$RuCl		−0.060				−1.30
1	−0.630	−0.285	0.345	6.80×10^5	0.70	−1.46
1−N$(CH_3)_2$	−0.690	−0.320	0.370	1.80×10^6	0.85	−1.50
1−NO_2	−0.585	−0.245	0.340	5.60×10^5	0.52	−1.47
2	−0.480	−0.310	0.170	748	0.59	−1.35
3	−0.360	−0.260	0.100	49	0.44	−1.38
4	−0.380	−0.020	0.360	1.22×10^6		−1.42
5	−0.520	−0.195	0.325	3.12×10^5		−1.49
6	−0.325	−0.220	0.105	60		−1.38
7	−0.405	−0.265	0.140	233		−1.44
8	−0.635	−0.385	0.250	1.68×10^4		−1.45
9	−0.175	0.070	0.245	1.39×10^4	1.00	−1.62
10	−0.060	0.070	0.130	158	0.661	−1.58
11	−0.068	0.002	0.070	15	0.61	−1.55
12[f]	0.105	0.220	0.125	130	0.94	−1.56
13[f]	0.205	0.290	0.085	27		−1.64
14	0.030	0.250	0.220	5.24×10^3		−1.59
15	0.145	0.235	0.090	33		−1.60
16	0.070	0.365	0.295	9.70×10^4		−1.63
17[g]	−0.185	−0.020	0.165	616		−1.91

[a] Potential data in volts vs Fc^+/Fc are from single scan cyclic voltammograms recorded at 25 °C in 0.1 M dichloromethane solution of $(Bu_4N)(PF_6)$. Detailed experimental conditions are given in the Experimental Section. [b] $\Delta E_{1/2} = E_{1/2}(B) - E_{1/2}(A)$ denotes the potential difference between redox processes A and B. [c] The comproportionation constants, K_c, were calculated by the formula $K_c = \exp(\Delta E_{1/2}/25.69)$ at 298 K.[50] [d] Oxidation potential of the thienyl in the bridging ligand. [e] Irreversible reduction of the chelating ligand. [f] Ruthenium-based redox processes are quasireversible. [g] The data is from ref 37.

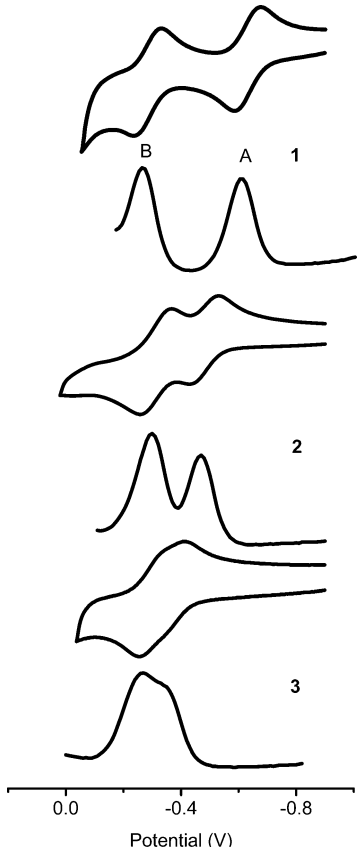

Figure 2. Cyclic and differential pulse voltammograms (CV and DPV) of compounds **1**−**3** in 0.1 M $(Bu_4N)(PF_6)$−dichloromethane solution. The scan rate is 100 mV s^{-1} for CV and 20 mV s^{-1} for DPV.

(50) Richardson, D. E.; Taube, H. *Inorg. Chem.* **1981**, *20*, 1278.

of the thiophene-centered oxidation depend strongly on the length of the oligothiophene spacers. With extension of the conjugation length by increasing thiophene units in the diethynyloligothiophenes, the oxidation potential is lowered progressively together with better reversibility.[42]

The $\Delta E_{1/2}$ values in **5**−**7** are 0.325, 0.105, and 0.140 V with the corresponding K_c being 3.12×10^5, 60, and 233, respectively, suggesting that successive insertion of 1,4-phenylene moieties into diynediyl induces a rapid decay of electronic communication from **5** to **6**.[38a,c] Interestingly, the $\Delta E_{1/2}$ value in **7** with 2,7-diethynylfluorene is obviously larger than that in **6** with 4,4′-diethynylbiphenyl, demonstrating distinctly that the rigid fluorene spacer is more favorable for electron transfer than the free rotatable 4,4′-biphenyl unit although the two symmetry-related 1,4-phenylene groups of **6** are coplanar in the solid state as revealed by X-ray crystallography (vide supra).

Although **1**, **4**, **5**, and **8** contain different types of polyynediyl bridges, the electronic interactions are mediated across the same nine bonds from one Ru center to the other. Since the $\Delta E_{1/2}$ and K_c values (Table 1) are **4** > **1** > **5** > **8**, electronic conduction capability for a series of π-conjugated carbon chains follows the sequence C≡C−(C≡C)$_2$−C≡C > C≡C(C_4H_2S)C≡C > C≡C(C_6H_4)C≡C > C≡C−(CH═CH)$_2$−C≡C. Similarly, by comparison of the $\Delta E_{1/2}$ and K_c values in **2**, **6**, and **7**, it is found that electronic interactions through the same 13 bonds between two Ru centers in molecular wires accord with **2** > **7** > **6**. This verifies unambiguously that insertion of 2,5-thiophene units into diynediyl is more favorable for electronic communication than that of the same number of 1,4-phenylene moieties.

For (Phtpy)(PPh_3)$_2$Ru-containing species **9**−**17**, successive insertion of one (**9**), two (**10**), or three (**11**) thiophene units to diethynyl induces a gradual decrease of the $\Delta E_{1/2}$ with 0.245 V (**9**) > 0.130 V (**10**) > 0.070 V (**11**) in the same trend as observed in **1**−**3**. Likewise, introducing one (**14**) or two (**15**) 1,4-phenylene groups to diethynyl results in reducing the $\Delta E_{1/2}$ from 0.220 V in **14** to 0.090 V in **15**. By comparison of the $\Delta E_{1/2}$ in **9**, **10**, or **12** with those in the corresponding counterparts **14**, **15**, or **13**, it is distinctly demonstrated that 2,5-thiophene as a spacer is more favorable than 1,4-phenylene for metal−metal communication, agreeing well with the conclusion made from [(bph)(PPh_3)$_2$Ru]$^+$-containing complexes mentioned above. By comparison of the $\Delta E_{1/2}$ (Table 1) in **9**, **14**, **16**, and **17**[37] with electronic interaction transmitted across nine Ru−C and C−C bonds, it is further confirmed that the electron conveying capability for a series of bridging ligands is C≡C−(C≡C)$_2$−C≡C > C≡C(C_4H_2S)C≡C > C≡C(C_6H_4)C≡C > C≡C−(CH═CH)$_2$−C≡C. For **10**, **12**, **13**, and **15** with electronic communication mediated across 13 Ru−C and C−C bonds, the $\Delta E_{1/2}$ values are **10** ≈ **12** > **13** ≈ **15**, implying that the electron mediating capability for the bridging ligands is C≡C(C_4H_2S)$_2$C≡C ≈ (C≡C)$_2$(C_4H_2S)(C≡C)$_2$ > (C≡C)$_2$(C_6H_4)-(C≡C)$_2$ ≈ C≡C(C_6H_4)$_2$C≡C. As a result, it appears that the electron mediating effect by insertion of two 2,5-thiophene/1,4-phenylene units to diethynyl is nearly the same as that by introducing one 2,5-thiophene/1,4-phenylene spacer to bis-(1,3-butadiynyl).

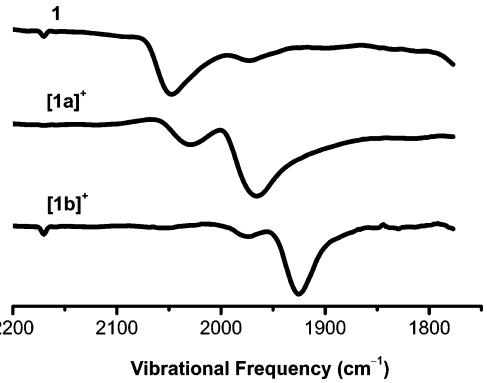

Figure 3. IR spectra of **1**, [**1a**]$^+$, and [**1b**]$^{2+}$ in solid states, showing the ν(C≡C) frequencies.

With careful examination of the electrochemical data listed in Table 1, it is intriguing to note that for two series of Ru_2 complexes with the same bridging C≡CRC≡C diynediyl but different ancillary chelating ligands, the $\Delta E_{1/2}$ and K_c of [(bph)(PPh_3)$_2$Ru]$^+$-containing complexes are significantly higher than those of the corresponding [(Phtpy)(PPh_3)$_2$Ru]$^+$-containing counterparts. This reveals distinctly that electron-rich bph is much more favorable for metal−metal electronic communication than electron-deficient Phtpy, possibly due to better energy matching of the dπ orbitals of the Ru center with the π* orbitals of the electron-rich bph. Additionally, it is noteworthy that the $\Delta E_{1/2}$ is tunable finely by modifying the substituent of phenyl (Scheme 2) in the Schiff base bph. As shown in Table 1, the $\Delta E_{1/2}$ of **1** (0.345 V) is larger than that of **1**−NO_2 (0.340 V) with electron-withdrawing −NO_2 but smaller than that of **1**−$N(CH_3)_2$ (0.370 V) with electron-donating −$N(CH_3)_2$. This reveals unambiguously that electronic communication is enhanced in some measure by introducing an electron-donating substituent to the phenyl of bph whereas reduced by an electron-attracting group.

IR Spectra. The ν(C≡C) stretching frequency in diyndiyl ligands is frequently useful to assess the rate of intramolecular electron transfer and the degree of electronic delocalization in the $Ru_2^{II,III}$ mixed-valence complexes.[20,38] As shown in Figure 3, the IR spectra in the $Ru_2^{II,III}$ mixed-valence complex [**1a**]$^+$ revealed two distinct C≡C stretching bands, while only a single ν(C≡C) stretching frequency is observed in the corresponding neutral $Ru_2^{II,II}$ complex **1** and dicationic $Ru_2^{III,III}$ species [**1a**]$^+$. The observation of two separate vibrational bands (Table S4, Supporting Information) for the $Ru_2^{II,III}$ mixed-valence complexes implies that the systems are not in the ideal cases with the odd electron fully delocalized along the rodlike backbone on the very rapid IR time scale (10^{-13} s),[38] probably due to the different electronic environment of the two acetylide bonds in the rodlike array Ru^{II}−C≡C(C_4H_2S)$_m$C≡C−Ru^{III}. Therefore, unobserved averaging of the C≡C vibrational modes for the $Ru_2^{II,III}$ complexes relative to the $Ru_2^{II,II}$ and $Ru_2^{III,III}$ species suggests that the mixed-valence complexes are not fully delocalized in the time scale of the IR spectrometry, and the electron transfer from the Ru^{II} to the Ru^{III} center is taking place at a rate constant of $<10^{13}$ s^{-1}.[43a] Furthermore, with

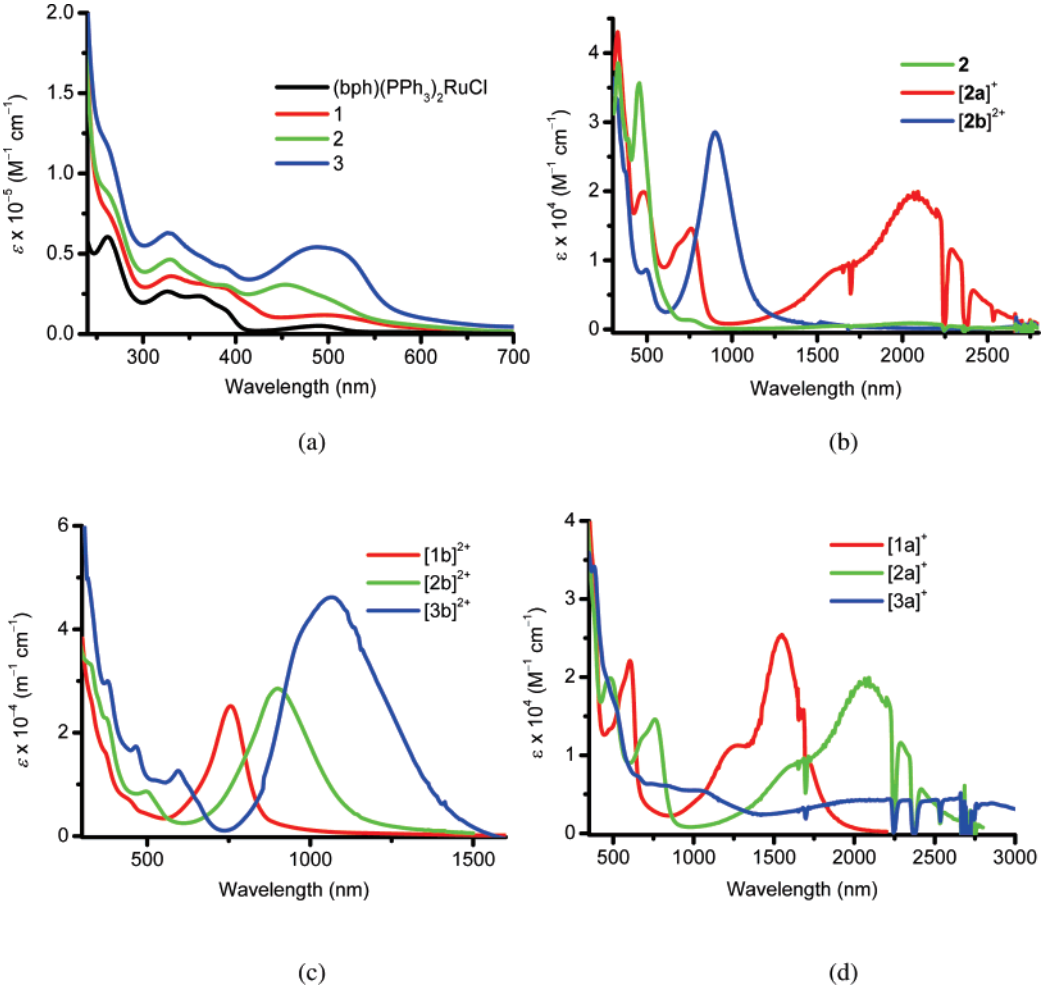

Figure 4. UV−vis−NIR spectra in dichloromethane: (a) (bph)$(PPh_3)_2$RuCl (black), **1** (red), **2** (green), and **3** (blue); (b) **2** (green), $[\mathbf{2a}]^+$ (red), and $[\mathbf{2b}]^{2+}$ (blue); (c) $Ru_2^{III,III}$ complexes $[\mathbf{1b}]^{2+}$ (red), $[\mathbf{2b}]^{2+}$ (green), and $[\mathbf{3b}]^{2+}$ (blue), showing the LMCT bands; (d) $Ru_2^{II,III}$ mixed-valence species $[\mathbf{1a}]^+$ (red), $[\mathbf{2a}]^+$ (green), and $[\mathbf{3a}]^+$ (blue), showing the IVCT bands.

stepwise one-electron oxidation of the neutral $Ru_2^{II,II}$ complexes into monocationic $Ru_2^{II,III}$ and dicationic $Ru_2^{III,III}$ species (Figure 3), a gradual lowering of the stretching frequency for the C≡C triple bonds demonstrates unambiguously a progressive increasing contribution from the cumulenic form.[23d,e,27,37]

UV−vis−NIR Spectra. The UV−vis−NIR absorption spectral data for $Ru_2^{II,II}$ complexes **1**−**17** and some $Ru_2^{II,III}$ and $Ru_2^{III,III}$ species are summarized in Table S5 (Supporting Information). For the purpose of comparison, the absorption spectra of **1**−**3**, $[\mathbf{2}]^{p+}$ (p = 0, **2**; 1, $[\mathbf{2a}]^+$; or 2, $[\mathbf{2b}]^{2+}$), $[\mathbf{1a}]^+$−$[\mathbf{3a}]^+$, and $[\mathbf{1b}]^{2+}$−$[\mathbf{3b}]^{2+}$ are depicted in Figure 4.

Intense absorption bands in the UV region for $Ru_2^{II,II}$ complexes **1**−**17** originate primarily from ligand-centered $\pi \rightarrow \pi^*$ transitions due to bph/Phtpy, PPh_3, and polyynediyl ligands. The broad absorptions in the visible region for $Ru_2^{II,II}$ complexes originate likely from dπ(Ru) → π^*(bph/Phtpy) MLCT (metal-to-ligand charge transfer) transitions. For thiophene-containing complexes **1**−**3** (Figure 4a) or **9**−**11** (Figure S4, Supporting Information), intense absorption bands due to the thiophene-based $\pi \rightarrow \pi^*$ transitions are observed in the range of 380−550 nm. As shown in Figure 4a and Figure S4 (Supporting Information), with the increase of thiophene units in the bridging ligands, not only is the energy of the transition red-shifted progressively but also the molar extinction coefficient is enhanced significantly.[42a,b]

Upon successive oxidation of thiophene-containing $Ru_2^{II,II}$ complexes **1**−**3** into $Ru_2^{II,III}$ species $[\mathbf{1a}]^+$−$[\mathbf{3a}]^+$ and $Ru_2^{III,III}$ species $[\mathbf{1b}]^{2+}$−$[\mathbf{3b}]^{2+}$, while the low-energy absorptions due to dπ(Ru) → π^*(bph) MLCT transition attenuate gradually in intensity, a new band with lower energy occurs in the visible to near-infrared region (Figure 4b), assigned tentatively to a ligand → Ru^{III} LMCT (ligand-to-metal charge transfer) transition induced by oxidation of Ru^{II} into $Ru^{I\text{-}II}$.[20,23,27,37] Similar low-energy absorptions due to thiophene ligand → M^{III} LMCT transitions have also been observed in other Ru^{III} or Fe^{III} complexes with conjugated oligothiophene ligands.[41,42] As shown in Figure 4b, the newly produced LMCT band shows a remarkable red shift from the monocationic $Ru_2^{II,III}$ complex $[\mathbf{2a}]^+$ (λ = 762 nm, ϵ = 14 760 M^{-1} cm^{-1}) to dicationic $Ru_2^{III,III}$ species $[\mathbf{2b}]^{2+}$ (λ = 900 nm, ϵ = 28 540 M^{-1} cm^{-1}) with the intensity enhanced significantly. By comparison of the absorption bands of the LMCT transitions for a series of dicationic $Ru_2^{III,III}$ complexes $[\mathbf{1b}]^{2+}$−$[\mathbf{3b}]^{2+}$ (Figure 4c), it is found that with the increase of thiophene units in the bridging ligands C≡C$(C_4H_2S)_m$C≡C, the absorption maxima shift significantly to the lower energy region with the intensity enhanced dramatically. This

Table 2. Visible−Near-Infrared Spectral Data for $Ru_2^{II,III}$ Mixed-Valence Complexes $[\mathbf{1a}]^+$−$[\mathbf{8a}]^+$ in Dichloromethane at 298 K

compound	λ_{max} (nm)	ϵ_{max} (cm^{-1} M^{-1})	ν_{max} (cm^{-1})	$\Delta\nu_{obsd}$ (cm^{-1})[a]	$\Delta\nu_{calcd}$ (cm^{-1})[b]	V_{ab} (eV)[c]	V_{ab}' (eV)[d]
$[\mathbf{1a}]^+$	1549	25400	6455	1310	2910	0.102	0.399
$[\mathbf{2a}]^+$	2092	19900	4780	1430	2810	0.061	0.296
$[\mathbf{3a}]^+$	2661	5150	3758	3900	2630	0.036	0.233
$[\mathbf{4a}]^+$	1575	23600	6349	1180	2820	0.083	0.393
$[\mathbf{5a}]^+$	1930	18100	5181	1210	2440	0.070	0.321
$[\mathbf{6a}]^+$	3078	3100	3248	2950	2350	0.027	0.201
$[\mathbf{7a}]^+$	3015	2000	3316	3310	2250	0.024	0.205
$[\mathbf{8a}]^+$	1562	10300	6402	1580	3180	0.066	0.396

[a] $\Delta\nu_{obsd}$ is the observed half-width of IVCT band. [b] $\Delta\nu_{calcd}$ is the calculated half-width from the equation $\Delta\nu_{1/2} = [2310(\nu_{max} - \nu_0)]^{1/2}$ by Hush's theoretical analysis, where ν_0 is estimated from the difference in the redox potentials $\Delta E_{1/2}$. [c] $V_{ab} = \{[(2.05 \times 10^{-2})(\nu_{max}\epsilon_{max}\Delta\nu_{1/2})^{1/2}]/R\}$ from Hush's theoretical analysis for a weakly coupling system of class II mixed-valence compounds, where ϵ_{max}, ν_{max}, and $\Delta\nu_{1/2}$ are the molar extinction coefficient, the absorption maximum in wavenumbers, and the observed bandwidth at half-maximum height in wavenumbers, respectively; the metal−metal distances R are 11.5, 15.3, 19.2, 12.8, 12.2, 16.5, 15.9, and 12.4 Å in $[\mathbf{1a}]^+$−$[\mathbf{8a}]^+$, respectively. [d] $V_{ab}' = \nu_{max}/2$ for electronically delocalized class III mixed-valence compounds.

reveals unambiguously that the energy maxima of these LMCT transitions are correlated to the length of the oligothiophene groups, in which the absorption is red-shifted and the intensity is enhanced with an extension of π-conjugation in the bridging ligands.[42a,b] As suggested by Wolf et al.,[42a,b] the absorption maximum of a charge-transfer band is correlated to the difference in electrochemical potentials between oligothiophene (donor) and metal (acceptor) for the LMCT transition in Ru^{III} complexes. A smaller difference in donor and acceptor oxidation potentials usually induces a larger oscillator strength and lower absorption maximum for the LMCT transitions. As the oxidation potential differences between oligothiophene (donor) and ruthenium (acceptor) are 0.988, 0.903, and 0.705 V for **1**, **2** and **3**, respectively, it is reasonable that with successive extension of the oligothiophene spacer in **1**−**3**, the LMCT peak strength is enhanced progressively whereas the absorption energy is lowered gradually.

The most significant absorption feature in a series of $Ru_2^{II,II}$, $Ru_2^{II,III}$, and $Ru_2^{III,III}$ species is the appearance of NIR absorption induced by $Ru^{II} \rightarrow Ru^{III}$ intervalence charge transfer (IVCT) transitions in the $Ru_2^{II,III}$ mixed-valence complexes, which are absent in the $Ru_2^{II,II}$ complexes and disappear entirely in the $Ru_2^{III,III}$ species as indicated in Figure 4b for **2**, $[\mathbf{2a}]^+$, and $[\mathbf{2b}]^{2+}$. Analyses of these IVCT absorptions (Table 2) give a series of decisive information on charge distribution and electronic delocalization in the monocationic $Ru_2^{II,III}$ mixed-valence complexes $[\mathbf{1a}]^+$−$[\mathbf{8a}]^+$. Figure 4d depicts the visible to near-infrared absorption spectra of thiophene-containing mixed-valence species $[\mathbf{1a}]^+$−$[\mathbf{3a}]^+$ measured in dichloromethane. Interestingly, with successive insertion of 2,5-thiophene units in the bridging ligands, IVCT bands of $[\mathbf{1a}]^+$−$[\mathbf{3a}]^+$ are gradually red-shifted in absorption position, increasingly broadened in shape, and progressively weakened in intensity. As found in many other mixed-valence compounds,[22a,35,38a,43a] the NIR spectra of $[\mathbf{1a}]^+$−$[\mathbf{3a}]^+$ exhibit a relative sharp IVCT absorption band together with a higher energy shoulder, induced probably by HOMO-1 to SOMO (singly occupied molecular orbital) transition.[20a,23a,38]

For $[\mathbf{1a}]^+$, an intense IVCT absorption occurs at λ_{max} = 1549 nm with a molar extinction coefficient ϵ = 25 400 cm^{-1} M^{-1}. Solvent independence of the IVCT absorption maximum λ_{max} in the solvents such as dichloromethane, acetonitrile, acetone, and methanol with a wide range of polarity is indicative of an average solvation (Figure S5, Supporting Information). The observed half-width $\Delta\nu_{1/2}$ (1310 cm^{-1}) is significantly narrower than the one (2910 cm^{-1}) calculated by the equation $\Delta\nu_{1/2} = [2310(\nu_{max} - \nu_0)]^{1/2}$ according to Hush theory.[12] Consequently, in view of the considerably large $\Delta E_{1/2}$ (0.345 V) and K_c (6.80×10^5), a high molar extinction coefficient ϵ (25 400 cm^{-1} M^{-1}) of the IVCT band, solvent independence of the IVCT absorption λ_{max}, and the narrow half-width ($\Delta\nu_{1/2}$), but being not fully delocalized in the time scale of the IR spectrometry, it is concluded that $[\mathbf{1a}]^+$ is probably close to valence-untrapped and classified tentatively as class II−III mixed-valence complex.[8,9,12] On the contrary, $[\mathbf{3a}]^+$ is unstable in acetonitrile, acetone, and methanol, and its IVCT band in dichloromethane is quite broad and relatively weak (ϵ = 5150 cm^{-1} M^{-1}). The observed half-width $\Delta\nu_{1/2}$ (3900 cm^{-1}) of the IVCT band is much broader than that (2630 cm^{-1}) predicted by Hush theory.[12] These features together with a small $\Delta E_{1/2}$ (0.100 V) and low comproportionation constant (K_c = 49) indicate that $[\mathbf{3a}]^+$ is typical of a valence-trapped system and can be classified as a class II mixed-valence complex[8,9] with weak electronic coupling between the Ru^{II} and Ru^{III} centers. For $[\mathbf{2a}]^+$, however, the IVCT features together with its stepwise redox potential difference $\Delta E_{1/2}$ are intermediate to those of $[\mathbf{1a}]^+$ and $[\mathbf{3a}]^+$, implying that the mixed-valence behavior is between class II−III and class II with partial electronic delocalization.[8] Consequently, both the IVCT absorption and electrochemical features in the $Ru_2^{II,III}$ mixed-valence complexes $[\mathbf{1a}]^+$−$[\mathbf{3a}]^+$ demonstrate unambiguously that a progressive transition from almost electronic delocalization (class II−III) to localization (class II) occurs according to the sequence $[\mathbf{1a}]^+ \rightarrow [\mathbf{2a}]^+ \rightarrow [\mathbf{3a}]^+$. As indicated in Table 2, the electronic coupling constants calculated by the equation $V_{ab} = \{[(2.05 \times 10^{-2})(\nu_{max}\epsilon_{max}\Delta\nu_{1/2})^{1/2}]/R\}$ (for class II mixed-valence complex) or $V_{ab}' = \nu_{max}/2$ (for class III mixed-valence complex)[21d,23d] are reduced dramatically according to the sequence $[\mathbf{1a}]^+ > [\mathbf{2a}]^+ > [\mathbf{3a}]^+$ with successive insertion of thiophene units to the bridging ligands.

Similarly, as inferred from both electrochemical and IVCT spectral data, a transition from almost electronic delocalization to localization occurs also in $[\mathbf{5a}]^+ \rightarrow [\mathbf{6a}]^+$ with a successive increase of 1,4-phenylene units in the bridging ligands.[38a] $[\mathbf{5a}]^+$ exhibits strong IVCT absorptions that are independent of the solvents such as dichloromethane, acetonitrile, acetone, and methanol. The observed half-width $\Delta\nu_{1/2}$ (1210 cm^{-1} in dichloromethane) of the IVCT band is much narrower than that (2440 cm^{-1}) predicted by Hush theory. $[\mathbf{6a}]^+$, however, is unstable in other solvents except dichloromethane, and its IVCT absorption (ϵ = 3100 cm^{-1} M^{-1}) is significantly weaker than that of $[\mathbf{5a}]^+$ (ϵ = 18 100

cm^{-1} M^{-1}). As presented in Table 2, the coupling constant V_{ab} or V_{ab}' of **5** is much higher than that of **6**.

For $Ru_2^{II,III}$ mixed-valence complexes [**4a**]$^+$, [**5a**]$^+$, and [**8a**]$^+$ with intramolecular electron-transfer mediated across nine Ru−C and C−C bonds from Ru^{II} to Ru^{III} centers, intense and solvent-independent IVCT absorptions are observed with the band maxima at 1575 (ϵ = 23 600 cm^{-1} M^{-1}), 1930 (ϵ = 18 100 cm^{-1} M^{-1}), and 1562 nm (ϵ = 10 300 cm^{-1} M^{-1}), respectively. As listed in Table 2, the half-widths $\Delta\nu_{1/2}$ are much narrower than those calculated by Hush theory. These features together with the considerably large $\Delta E_{1/2}$ and K_c values suggest that they are likely class II−III or intermediate between class II−III and class II mixed-valence complexes.

Magnetic Susceptibility. The room-temperature magnetic moments of $[Ru_2^{II,III}]^+$ species [**1a**]$^+$, [**2a**]$^+$, and [**3a**]$^+$ are 1.78, 1.82, and 1.87 μ_B at 300 K, respectively, and demonstrated unambiguously that they are typical of a single unpaired electron. Variable-temperature magnetic susceptibilities were measured on powdered samples of [**1b**]$^{2+}$−[**3b**]$^{2+}$ (Figure S6). The effective magnetic moments are 2.84, 2.69, and 2.60 μ_B for [**1b**]$^{2+}$, [**2b**]$^{2+}$, and [**3b**]$^{2+}$ at 300 K, respectively, indicating that the compounds have two unpaired electrons although the values are a little higher than those expected for the spin-only values of two unpaired-electron species. For [**1b**]$^{2+}$, the value of μ_{eff} decreased slightly with decreasing temperature (1.98 μ_B at 35 K). Below 35 K, the μ_{eff} decreased rapidly and reached 1.25 μ_B at 2 K. Similar behavior is observed for [**2b**]$^{2+}$ and [**3b**]$^{2+}$. As [**1b**]$^{2+}$−[**3b**]$^{2+}$ with different lengths of bridging ligands exhibit similar temperature-dependent magnetic behavior, the decrease of μ_{eff} with a decrease of temperatures is likely due to considerably large Ru^{III} spin−orbit splitting of the $^2T_{2g}$ ground term instead of the pure spin coupling.[51]

Conclusions

Designed syntheses of a series of wirelike ruthenium-capped polyynediyl complexes have been achieved by reaction of (bph)$(PPh_3)_2$RuCl or [(Phtpy)$(PPh_3)_2$Ru(acetone)]$(ClO_4)_2$ with $Me_3Si-C\equiv C-R-C\equiv C-SiMe_3$ via fluoride-catalyzed desilylation. Controlling the oxidation of bis(ethynyl)oligothiophene connected diruthenium $Ru_2^{II,II}$ complexes induces the isolation of stable monoanionic $[Ru_2^{II,III}]^+$ and dianionic $[Ru_2^{III,III}]^{2+}$ species in the solid state, respectively. With stepwise oxidation of thiophene-containing $Ru_2^{II,II}$ complexes into $[Ru_2^{II,III}]^+$ and $[Ru_2^{III,III}]^{2+}$ species, while the MLCT absorption attenuates and disappears gradually, lower energy LMCT absorption occurs, intensifies, and red-shifts progressively. It is revealed that the energy maxima of these LMCT transitions are correlated to the length of the oligothiophene groups, in which the absorption is red-shifted and the intensity is enhanced with an extension of π-conjugation in the bridging ligands by increasing thiophene spacers. From UV−vis−NIR spectral studies, it is demonstrated unambiguously that with successive insertion of thiophene groups in the bis(ethynyl)oligothiophene ligands, intramolecular electron transfer is reduced progressively with a smooth transition from almost electronic delocalization to localization. It is intriguing that (bph)$(PPh_3)_2$Ru-containing wirelike species are much more favorable for electronic communication than that of (Phtpy)$(PPh_3)_2$Ru-containing ones. Tuning intramolecular electron transfer by modification of the ancillary ligands indicates that introducing an electron-donating substituent favors intermetallic electronic communication whereas an electron-withdrawing one attenuates intermetallic electronic communication. In a series of mixed-valence diruthenium complexes with intramolecular electron transfer mediated across nine Ru−C and C−C bonds, the conveying capability for the bridging ligands is $C\equiv C(C\equiv C)_2C\equiv C$ > $C\equiv C(C_4H_2S)C\equiv C$ > $C\equiv C(C_6H_4)C\equiv C$ > $C\equiv C(CH=CH)_2C\equiv C$.

Experimental Section

General Materials. All operations were performed under argon atmosphere using Schlenk techniques and vacuum-line systems. Solvents were dried by standard methods and distilled prior to use except that those for UV−vis−NIR spectral measurements were of spectroscopic grade. The reagents ruthenium(III) chloride hydrate, picolinaldehyde, benzoylhydrazine, triphenylphosphine (PPh_3), 1,4-bis(ethynyl)benzene ($HC\equiv C(C_6H_4)C\equiv CH$), and ferrocenium hexafluorophosphate ($(Cp_2Fe)(PF_6)$) were commercially available (Alfa Aesar). The compounds (bph)$(PPh_3)_2$RuCl (bph = *N*-(benzoyl)-*N*′-(picolinylidene)hydrazine),[46] 4′-phenyl-2,2′:6′,2″-terpyridine (Phtpy),[52a] [(Phtpy)$(PPh_3)_2$RuCl]−(ClO_4),[52b] 2,5-bis(trimethylsilylethynyl)thiophene ($Me_3SiC\equiv C(C_4H_2S)C\equiv CSiMe_3$),[44a,] 5,5′-bis(trimethylsilylethynyl)-2,2′-bithiophene ($Me_3SiC\equiv C(C_4H_2S)_2C\equiv CSiMe_3$),[44a,b] 5,5″-bis(trimethylsilylethynyl)-2,2′:5′,2″-terthiophene ($Me_3Si-C\equiv C(C_4H_2S)_3C\equiv CSiMe_3$),[44a] (*E*)-$Me_3SiC\equiv C-CH=CH-C\equiv CSiMe_3$,[53] 1,8-bis(trimethylsilanyl)octa-1,3,5,7-tetrayne ($Me_3SiC\equiv CC\equiv CC\equiv C-C\equiv CSiMe_3$),[54] 4,4′-bis(trimethylsilyethynyl)-biphenyl ($Me_3SiC\equiv C(C_6H_4)_2C\equiv CSiMe_3$),[55] and 2,7-bis(trimethylsilyethynyl)fluorene ($Me_3SiC\equiv C(C_6H_3CH_2C_6H_5)-C\equiv CSiMe_3$)[56] were prepared by the procedures described in literature procedures. 2,5-Bis[(trimethylsilyl)-1,3-butadiynyl]thiophene ($Me_3SiC\equiv CC\equiv C(C_4H_2S)C\equiv CC\equiv CSiMe_3$) and 1,4-bis[(trimethylsilyl)-1,3-butadiynyl]benzene ($Me_3SiC\equiv CC\equiv C(C_6H_4)C\equiv CC\equiv CSiMe_3$) were synthesized by $Pd(PPh_3)_2Cl_2$/CuI-catalyzed cross-coupling reactions of 1,4-dibromobenzene or 2,5-dibromothiophene with an excess of trimethylsilylbutadiyne ($Me_3SiC\equiv CC\equiv CH$), analogous to the Sonogashira coupling reactions.[55] Compound **17** was reported in ref 37.

{(bph)$(PPh_3)_2$Ru}$_2${C≡C(C_4H_2S)C≡C} (1) and [{(bph)$(PPh_3)_2$Ru}$_2${C≡C-(C_4H_2S)-C≡C}](PF_6) ([1a](PF_6)). To 60 mL of methanol were added (bph)$(PPh_3)_2$RuCl (300 mg, 0.34 mmol), 2,5-bis(trimethylsilylethynyl)thiophene (47 mg, 0.17 mmol), and potassium fluoride (25 mg, 0.42 mmol) with stirring. After the solution was refluxed for 1 day, the solvents were removed in vacuo,

(51) Bai, L. X.; Liu, X.; Wang, W. Z.; Liao, D. Z.; Wang, Q. L. *Z. Anorg. Allg. Chem.* **2004**, *630*, 1143.

(52) (a) Constable, E. C.; Lewis, J.; Liptrot, M. C.; Raithby, P. R. *Inorg. Chim. Acta* **1990**, *178*, 47. (b) Sullivan, B. P.; Calvert, J. M.; Meyer, T. J. *Inorg. Chem.* **1980**, *19*, 1404.

(53) Walker, J. A.; Bitler, S. P.; Wudl, F. *J. Org. Chem.* **1984**, *49*, 4733.

(54) Eastmond, R.; Johnson, T. R.; Walton, D. R. M. *Tetrahedron* **1972**, *28*, 4601.

(55) (a) Tohda, Y.; Sonogashira, K.; Hagihara, N. *Synthesis* **1977**, 777. (b) Sonogashira, K.; Tohda, Y.; Hagihara, N. *Tetrahedron Lett.* **1975**, *16*, 4467.

(56) Lewis, J.; Raithby, P. R.; Wong, W.-Y. *J. Organomet. Chem.* **1998**, *556*, 219.

and the residue was dissolved in dichloromethane. After filtration, the solution was chromatographed on a basic alumina column. The brown band was eluted with dichloromethane to give the neutral product **1**. Elution of the blue band with dichloromethane afforded the mixed-valence compound [**1a**](PF_6) by addition of a methanol solution of ammonium hexafluorophosphate.

1. Yield: 21%. Anal. Calcd for $C_{106}H_{82}N_6O_2P_4Ru_2S$: C, 69.57; H, 4.52; N, 4.59. Found: C, 69.31; H, 4.32; N 4.45. ESI-MS: *m*/*z* (%) 1830 (100) $[M]^+$, 1567 (8) $[M - PPh_3]^+$, 588 (20) [(bph)-(PPh_3)Ru]$^+$. IR spectrum (KBr, cm^{-1}): ν 2047 m (C≡C). ^1H NMR spectrum ($CDCl_3$, ppm): δ 7.72 (s, 2H, HC═N), 7.53−7.20 (m, 78H, C_5H_4N and C_6H_5), 6.84 (s, 2H, C_4H_2S). ^{31}P NMR spectrum ($CDCl_3$, ppm): δ 30.8 (s).

[1a](PF$_6$). Yield: 41%. Anal. Calcd for $C_{106}H_{82}F_6N_6O_2P_5Ru_2S$: C, 64.47; H, 4.19; N, 4.26. Found: C, 64.26; H, 4.22; N 4.27. ESI-MS: *m*/*z* (%) 1974 (1) $[M]^+$, 1830 (100) $[M - (PF_6)]^+$, 588 (20) [(bph)(PPh_3) Ru]$^+$. IR spectrum (KBr, cm^{-1}): ν 2029 m (C≡C), 1966 s (C≡C), 839 s (PF_6). ^{31}P NMR spectrum ($CDCl_3$): δ 28.3 (s), −144.6 (septet, *P*F_6).

[{(bph)(PPh$_3$)$_2$Ru}$_2${C≡C(C$_4$H$_2$S)C≡C}](PF$_6$)$_2$ ([1b](PF$_6$)$_2$). To a dichloromethane (20 mL) solution of **1** (95 mg, 0.052 mmol) was added ferrocenium hexafluorophosphate (33 mg, 0.10 mmol) with the color changing from brown to green. After being stirred at room temperature for 1 h, the solution was concentrated to 3 mL by evaporation of the solvent. Diethyl ether was added to the concentrated solution to precipitate the product which was washed with diethyl ether three times to give the pure compound. Yield: 76%. Anal. Calcd for $C_{106}H_{82}F_{12}N_6O_2P_6Ru_2S$: C, 60.06; H, 3.90; N, 3.96. Found: C, 60.24; H, 4.04; N, 4.07. ESI-MS: *m*/*z* (%) 915 (100) $[M - (PF_6)_2]^{2+}$, 850 (90) $[(bph)(PPh_3)_2Ru]^+$. IR spectrum (KBr, cm^{-1}): ν 1923 m (C≡C), 838 s (PF_6). ^{31}P NMR spectrum (CH_2Cl_2): δ 23.7 (s), −144.6 (septet, *P*F_6).

{(bph−N(CH$_3$)$_2$)(PPh$_3$)$_2$Ru}$_2${C≡C(C$_4$H$_2$S)C≡C} (1−N(CH$_3$)$_2$). This compound was prepared by the same procedure as that of **1** except using (bph-N(CH_3)$_2$)(PPh_3)$_2$RuCl instead of (bph)(PPh_3)$_2$-RuCl. The product was purified on a neutral alumina column by chromatography to collect the second brown band using dichloromethane−*n*-hexane (1:2) as an eluent. Yield: 35%. Anal. Calcd for $C_{110}H_{92}N_8O_2P_4Ru_2S$: C, 68.95; H, 4.84; N, 5.85. Found: C, 69.01; H, 4.88; N, 5.74. ESI-MS: *m*/*z* (%) 1916 (100) $[M]^+$, 1653 (35) $[M - PPh_3]^+$, 1392 (10) $[M - (PPh_3)_2]^+$, 893 (10) [(bph-N(CH_3)$_2$)(PPh_3)$_2$Ru]$^+$, 631 (80) [(bph-N(CH_3)$_2$)(PPh_3)Ru]$^+$. IR spectrum (KBr, cm^{-1}): ν 2034 m (C≡C). ^1H NMR spectrum ($CDCl_3$, ppm): δ 7.74 (s, 2H, HC═N), 7.48−7.26 (m, 76H, C_5H_4N and C_6H_5), 6.45 (s, 2H, C_4H_2S), 2.98 (s, 12H, CH_3). ^{31}P NMR spectrum (CH_2Cl_2): δ 32.4 (s).

{(bph−NO$_2$)(PPh$_3$)$_2$Ru}$_2${C≡C(C$_4$H$_2$S)C≡C} (1−NO$_2$). This compound was prepared by the same procedure as that of **1** except using (bph−NO_2)(PPh_3)$_2$RuCl instead of (bph)(PPh_3)$_2$RuCl. The product was purified on a neutral alumina column by chromatography to collect the second brown band using dichloromethane−*n*-hexane (1:2) as an eluent. Yield: 48%. Anal. Calcd for $C_{106}H_{80}N_8O_6P_4Ru_2S$: C, 66.31; H, 4.20; N, 5.84. Found: C, 66.45; H, 4.27; N, 5.80. ESI-MS: *m*/*z* (%) 1920 (100) $[M]^+$, 1658 (5) [M − PPh_3]. IR spectrum (KBr, cm^{-1}): ν 2038 m (C≡C). ^1H NMR spectrum ($CDCl_3$, ppm): δ 7.98 (s, 2H, HC═N), 7.53−6.86 (m, 76H, C_6H_4N and C_6H_5), 6.77 (s, 2H, C_4H_2S). ^{31}P NMR spectrum (CH_2Cl_2): δ 32.6 (s).

{(bph)(PPh$_3$)$_2$Ru}$_2${C≡C(C$_4$H$_2$S)$_2$C≡C} (2). This compound was prepared by the same procedure as that of **1** except using 5,5′-bis(trimethylsilylethynyl)-2,2′-bithiophene instead of 2,5-bis(trimethylsilylethynyl)thiophene. The product was purified on a neutral alumina column by chromatography to collect the second brown band using dichloromethane−*n*-hexane (1:2) as an eluent. Yield: 48%. Anal. Calcd for $C_{110}H_{84}N_6O_2P_4Ru_2S_2$: C, 69.10; H, 4.43; N, 4.40. Found: C, 69.39; H, 4.29; N, 4.64. ESI-MS: *m*/*z* (%) 1913 (100) $[M]^+$, 850 (60) $[(bph)(PPh_3)_2Ru]^+$, 588 (30) [(bph)(PPh_3)-Ru]$^+$. IR spectrum (KBr, cm^{-1}): ν 2038 w (C≡C). ^1H NMR spectrum ($CDCl_3$, ppm): δ 7.72 (s, 2H, HC═N), 7.53−7.18 (m, 78H, C_5H_4N and C_6H_5), 7.10 [d, 2H, $^3J(H^4H^3)$ or $(H^{4'}H^{3'})$= 8 Hz, $H^{4,4'}$], 6.82 [d, 2H, $^3J(H^3H^4)$ or $(H^{3'}H^{4'})$= 8 Hz, $H^{3,3'}$]. ^{31}P NMR spectrum ($CDCl_3$): δ 32.8 (s).

[{(bph)(PPh$_3$)$_2$Ru}$_2${C≡C(C$_4$H$_2$S)$_2$C≡C}](PF$_6$) ([2a](PF$_6$)). To a dichloromethane (20 mL) solution of **2** (100 mg, 0.052 mmol) was added ferrocenium hexafluorophosphate (17 mg, 0.052 mg) with stirring at room temperature for 1 h. Diethyl ether was added to the concentrated solution to precipitate the deep brown product which was filtrated, washed with diethyl ether, and dried in vacuo. Yield: 95%. Anal. Calcd for $C_{110}H_{84}F_6N_6O_2P_5Ru_2S_2$: C, 64.23; H, 4.12; N, 4.09. Found: C, 64.57; H, 4.28; N, 3.89. ESI-MS (*m*/*z*): 1912 (95) $[M - PF_6]^+$, 588 (32) $[(bph)(PPh_3)Ru]^+$. IR spectrum (KBr, cm^{-1}): ν 1974 s (C≡C), 1936 s (C≡C), ν 838 s (PF_6). ^{31}P NMR spectrum (CH_2Cl_2): δ 28.5 (s), −144.6 (septet, *P*F_6).

[{(bph)(PPh$_3$)$_2$Ru}$_2${C≡C(C$_4$H$_2$S)$_2$C≡C}](PF$_6$)$_2$ ([2b](PF$_6$)$_2$). The synthetic procedure of this compound is the same as that of [**1b**](PF_6)$_2$ using **2** instead of **1**. Yield: 87%. Anal. Calcd for $C_{110}H_{84}F_{12}N_6O_2P_6Ru_2S_2$: C, 60.00; H, 3.85; N, 3.82. Found: C, 60.36; H, 3.90; N, 3.92. ESI-MS (*m*/*z*): 956 (100) $[M]^{2+}$, 693 (40) $[M - 2PPh_3]^{2+}$, 588 (10) $[(bph)(PPh_3)Ru]^+$. IR spectrum (KBr, cm^{-1}): ν 1910 m (C≡C), 838 (PF_6). ^{31}P NMR spectrum (CH_2Cl_2): δ 24.0 (s), −144.6 (septet, *P*F_6)

{(bph)(PPh$_3$)$_2$Ru}$_2${C≡C(C$_4$H$_2$S)$_3$C≡C} (3). This compound was prepared by the same procedure as that of **1** except using 5,5″-bis(trimethylsilylethynyl)-2,2′:5′,2″-terthiophene instead of 2,5-bis-(trimethylsilylethynyl)thiophene. The product was purified on a neutral alumina column by chromatography to collect the second red band using dichloromethane−*n*-hexane (1:2) as an eluent. Yield: 57%. Anal. Calcd for $C_{114}H_{86}N_6O_2P_4Ru_2S_3$: C, 68.66; H, 4.35; N, 4.21. Found: C, 69.01; H, 4.34; N, 3.92. ESI-MS(*m*/*z*): 1994 (100) $[M]^+$, 1732 (20) $[M - PPh_3]^+$ 1470 (10) $[M - (PPh_3)_2]^+$ 850 (30) $[(bph)(PPh_3)_2Ru]^+$, 588 (40) $[(bph)(PPh_3)Ru]^+$. IR spectrum (KBr, cm^{-1}): ν 2033 s (C≡C). ^1H NMR spectrum ($CDCl_3$, ppm): δ 7.69 (s, 2H, HC═N), 7.62−7.06 (m, 78H, C_5H_4N and C_6H_5), 7.12 (s, 2H, $H^{3',4'}$), 7.07 [d, 2H, $^3J(H^4H^3)$ or $(H^{4''}H^{3''})$= 7.5 Hz, $H^{4,4''}$], 6.83 [d, 2H, $^3J(H^3H^4)$ or $(H^{3''}H^{4''})$= 7.5 Hz, $H^{3,3''}$]. ^{31}P NMR spectrum ($CDCl_3$): δ 33.1 (s).

[{(bph)(PPh$_3$)$_2$Ru}$_2${C≡C(C$_4$H$_2$S)$_3$C≡C)}](PF$_6$) ([3a](PF$_6$)). Synthetic procedure of this compound is the same as that of [**2a**](PF_6) using **3** instead of **2**. Yield: 83%. Anal. Calcd for $C_{114}H_{86}F_6N_6O_2P_5Ru_2S_3$: C, 64.01; H, 4.05; N, 3.93. Found: C, 63.94; H, 4.25; N, 4.05. ESI-MS (*m*/*z*): 1994 (5) $[M - PF_6]^+$, 882 (100) $[\{(bph)(PPh_3)RuC{\equiv}C(C_4H_2S)_3C{\equiv}C\}]^+$, 588 (45) [(bph)-($PPh_3$)Ru]$^+$. IR spectrum (KBr, cm^{-1}): ν 2028 w (C≡C), 1974 m (C≡C), 838 (PF_6). ^{31}P NMR spectrum (CH_2Cl_2): δ 28.1 (s), −144.6 (septet, *P*F_6).

[{(bph)(PPh$_3$)$_2$Ru}$_2${C≡C(C$_4$H$_2$S)$_3$C≡C)}](PF$_6$)$_2$ ([3b](PF$_6$)$_2$). Synthetic procedure of this compound is the same as that of [**1b**](PF_6)$_2$ using **3** instead of **1**. Yield: 77%. Anal. Calcd for $C_{114}H_{86}F_{12}N_6O_2P_6Ru_2S_3$: C, 59.95; H, 3.80; N, 3.68. Found: C, 60.44; H, 3.81; N, 3.77. ESI-MS (*m*/*z*): 997 (100) $[M]^{2+}$, 588 (65) $[(bph)(PPh_3)Ru]^+$. IR spectrum (KBr, cm^{-1}): ν 1923 m (C≡C), 839 s (PF_6). ^{31}P NMR spectrum (CH_2Cl_2): δ 23.7 (s), −144.6 (septet, *P*F_6).

{(bph)(PPh$_3$)$_2$Ru}$_2$(C≡CC≡CC≡CC≡C) (4). This compound was prepared by the same procedure as that of **1** except using 1,8-bis(trimethylsilanyl)octa-1,3,5,7-tetrayne instead of 2,5-bis(trim-

ethylsilylethynyl)thiophene. The product was purified on a neutral alumina column by chromatography to collect the first modena band using dichloromethane−*n*-hexane (1:2) as an eluent. Yield: 35%. Anal. Calcd for $C_{106}H_{80}N_6O_2P_4Ru_2$: C, 70.89; H, 4.49; N, 4.68. Found: C, 70.83; H, 4.28; N, 4.54. ESI-MS (*m*/*z*): 1796 (100) $[M]^+$, 850 (5) $[(bph)(PPh_3)_2Ru]^+$. IR spectrum (KBr, cm^{-1}): ν 2106 m (C≡C), 1943 m (C≡C). ^1H NMR spectrum ($CDCl_3$, ppm): δ 7.59 (s, 2H, HC═N), 7.47−6.83 (m, 78H, C_5H_4N and C_6H_5). ^{31}P NMR spectrum ($CDCl_3$): δ 31.4 (s).

[{(bph)(PPh$_3$)$_2$Ru}$_2$(C≡CC≡CC≡CC≡C)](PF$_6$) ([4](PF$_6$)). The synthetic procedure of this compound is the same as that of [**2a**](PF_6) using **4** instead of **2**. Yield: 91%. Anal. Calcd for $C_{106}H_{80}F_6N_6O_2P_5Ru_2$: C, 65.60; H, 4.15; N, 4.33. Found: C, 65.11; H, 4.12; N, 4.27. ESI-MS (*m*/*z*): 1796 (100) $[M - PF_6]^+$, 1533 (56) $[M - PF_6 - (PPh_3)]^+$. IR spectrum (KBr, cm^{-1}): ν 2075 m (C≡C), 1893 m (C≡C). ^{31}P NMR spectrum (CH_2Cl_2): δ 28.2 (s), −144.8 (septet, PF_6).

{(bph)(PPh$_3$)$_2$Ru}$_2${C≡C(C$_6$H$_4$)C≡C} (5). (bph)(PPh_3)$_2$RuCl (300 mg, 0.34 mmol), 1,4-bis(ethynyl)benzene (22 mg, 0.17 mmol), and triethylamine (1 mL) were added to 60 mL of methanol with stirring, and the solution was refluxed for 1 day. The solvent was removed in vacuo, and the residue was chromatographed on a neutral alumina column. The brown product was collected as the second band using dichloromethane−*n*-hexane (1:2) as an eluent. Yield: 85%. Anal. Calcd for $C_{108}H_{84}N_6O_2P_4Ru_2$: C, 71.12; H, 4.64; N, 4.61. Found: C, 71.54; H, 4.51; N, 4.73. ESI-MS (*m*/*z*): 1824 (100) $[M]^+$, 1562 (3) $[M - PPh_3]^+$, 588 (5) $[(bph)(PPh_3)Ru]^+$. IR spectrum (KBr, cm^{-1}): ν 2056 m (C≡C). ^1H NMR spectrum ($CDCl_3$, ppm): δ 7.72 (s, 2H, HC═N), 7.59−7.16 (m, 82H, C_5H_4N, C_6H_5 and C_6H_4). ^{31}P NMR spectrum ($CDCl_3$): δ 33.0 (s).

[{(bph)(PPh$_3$)$_2$Ru}$_2${C≡C(C$_6$H$_4$)C≡C}](PF$_6$) ([5a](PF$_6$)). This compound was prepared by the same procedure as that of [**2a**](PF_6) using **6** instead of **2**. Yield: 93%. Anal. Calcd for $C_{108}H_{84}F_6N_6O_2P_5Ru_2 \cdot {}^1/_2CH_2Cl_2$: C, 64.79; H, 4.26; N, 4.18. Found: C, 64.23; H, 4.47; N, 4.32. ESI-MS (*m*/*z*): 1824 (20) $[M - PF_6]^+$, 588 (100) $[(bph)(PPh_3)Ru]^+$. IR spectrum (KBr, cm^{-1}): ν 2044 w (C≡C), 1973 s (C≡C), 839 (PF_6). ^{31}P NMR spectrum (CH_2Cl_2): δ 28.5 (s), −144.7 (septet, PF_6).

{(bph)(PPh$_3$)$_2$Ru}$_2${C≡C(C$_6$H$_4$)$_2$C≡C} (6). This compound was prepared by the same procedure as that of **1** except using 4,4′-bis(trimethylsilyethynyl)biphenyl instead of 2,5-bis(trimethylsilylethynyl)thiophene. The product was purified on a neutral alumina column by chromatography to collect the second brown band using dichloromethane−*n*-hexane (1:2) as an eluent. Yield: 71%. Anal. Calcd for $C_{114}H_{88}N_6O_2P_4Ru_2 \cdot H_2O$: C, 71.39; H, 4.73; N, 4.38. Found: C, 71.11; H, 4.59; N, 4.29. ESI-MS (*m*/*z*): 1900 (100) $[M]^+$, 1639 (25) $[M - PPh_3]^+$ 588 (40) $[(bph)(PPh_3)Ru]^+$. IR spectrum (KBr, cm^{-1}): ν 2057 m (C≡C). ^1H NMR spectrum ($CDCl_3$, ppm): δ 7.79 (s, 2H, HC═N), 7.58−6.83 (m, 86H, C_5H_4N, C_6H_5 and C_6H_4). ^{31}P NMR spectrum ($CDCl_3$): δ 32.7 (s).

{(bph)(PPh$_3$)$_2$Ru}$_2${C≡C(C$_6$H$_3$CH$_2$C$_6$H$_3$)C≡C} (7). This compound was prepared by the same procedure as that of **1** except using 2,7-bis(trimethylsilyethynyl)fluorene instead of 2,5-bis(trimethylsilylethynyl)thiophene. The product was purified on a neutral alumina column by chromatography to collect the second brown band using dichloromethane−*n*-hexane (1:2) as an eluent. Yield: 62%. Anal. Calcd for $C_{115}H_{88}N_6O_2P_4Ru_2$: C, 72.24; H, 4.64; N, 4.40. Found: C, 72.68; H, 4.53; N, 4.19. ESI-MS (*m*/*z*): 1912 (50) $[M]^+$, 588 (100) $[(bph)(PPh_3)Ru]^+$. IR spectrum (KBr, cm^{-1}): ν 2043 (C≡C). ^1H NMR spectrum ($CDCl_3$, ppm): δ 7.71 (s, 2H, HC═N)), 7.66−7.13 (m, 84H, C_5H_4N, C_6H_5 and C_6H_4), 4.09 (s, 2H, CH_2). ^{31}P NMR spectrum ($CDCl_3$): δ 33.1 (s).

{(bph)(PPh$_3$)$_2$Ru}$_2$(3*E*,5*E*-C≡CCH═CHCH═CHC≡C) (8). This compound was prepared by the same procedure as that of **1** except using (3*E*,5*E*)-$Me_3SiC{\equiv}C-CH{=}CH-CH{=}CH-C{\equiv}CSiMe_3$ instead of 2,5-bis(trimethylsilylethynyl)thiophene. The product was purified on a neutral alumina column by chromatography to collect the second brown band using dichloromethane−*n*-hexane (2:1) as an eluent. Yield: 57%. Anal. Calcd for $C_{106}H_{84}N_6O_2P_4Ru_2 \cdot {}^1/_2CH_2Cl_2$: C, 69.43; H, 4.65; N, 4.56. Found: C, 69.72; H, 4.73; N, 4.71. ESI-MS (*m*/*z*): 1800 (100) $[M]^+$, 588 (35) $[(bph)(PPh_3)Ru]^+$. IR spectrum (KBr, cm^{-1}): ν 2017 m (C≡C), 1636 m (C═C). ^1H NMR spectrum ($CDCl_3$, ppm): δ 7.64 (s, 2H, HC═N), 7.46−7.24 (m, 78H, C_5H_4N, C_6H_5), 6.97 (m, 2H, C≡C−CH═C*H*−C*H*═CH−C≡C), 6.65 (m, 2H, C≡C−C*H*═CH−CH═C*H*−C≡C). ^{31}P NMR spectrum ($CDCl_3$): δ 34.1 (s).

[{(bph)(PPh$_3$)$_2$Ru}$_2${3*E*,5*E*-C≡CCH═CHCH═CHC≡C}](PF$_6$) ([8a](PF$_6$)). This compound was prepared by the same procedure as that of [**2a**](PF_6) using **8** instead of **2**. Yield: 87%. Anal. Calcd for $C_{106}H_{84}N_6F_6O_2P_5Ru_2$: C, 65.46; H, 4.35; N, 4.32. Found: C, 66.01; H, 4.30; N, 4.41. ESI-MS (*m*/*z*): 1800 (67) $[M - PF_6]^+$, 850 (100) $[(bph)(PPh_3)_2Ru]^+$. IR spectrum (KBr, cm^{-1}): ν 1956 (C≡C), 840 (PF_6). ^{31}P NMR spectrum (CH_2Cl_2): δ 27.8 (s), −144.8 (septet, PF_6).

[{(Phtpy)(PPh$_3$)$_2$Ru}$_2$(C≡C(C$_4$H$_2$S)C≡C)](ClO$_4$)$_2$ (9). [(Phtpy)(PPh_3)$_2$RuCl](ClO_4) (150 mg, 0.14 mmol) and silver perchlorate (30.0 mg, 0.14 mmol) were dissolved in acetone (50 mL). After the solution was stirred under reflux for half an hour, it was cooled to room temperature and filtered to remove the silver chloride precipitate. To the brown filtrate were added 2,5-bis(trimethylsilylethynyl)thiophene (20.0 mg, 0.07 mmol) and potassium fluoride (10 mg, 0.17 mmol). The solution was then stirred under reflux for 1 day to become deep brown. The product was purified by chromatography on a neutral alumina column using dichloromethane−acetone (10:1) as an eluent to collect the second band. Yield: 80%. Anal. Calcd for $C_{122}H_{92}Cl_2N_6O_8P_4Ru_2S$: C, 66.63; H, 4.22; N, 3.82. Found: C, 66.45; H, 4.30; N, 3.88. ESI-MS: *m*/*z* (%) 1065 (40) $[\{(Phtpy)(PPh_3)_2Ru\ C{\equiv}C(C_4H_2S)C{\equiv}C\}]^+$, 1000 (100) $[M - (ClO_4)_2]^{2+}$, 673 (50) $[\{(Phtpy)(PPh_3)Ru\}]^+$. IR spectrum (KBr, cm^{-1}): ν 2042 m (C≡C), 1089 s (ClO_4). ^1H NMR spectrum (CD_3CN, ppm): δ 8.81 (d, 4H, J = 7.5 Hz, tpy(66″)), 8.01 (d, 4H, J = 7.5 Hz, tpy(33″)), 7.81 (d of d, 4H, J = 11.5 Hz, J' = 7.5 Hz, tpy(44″)), 7.69 (s, 4H, tpy(3′5′)), 7.62−7.09 (m, 70H, C_6H_5, and 4H, tpy (55″)), 7.0 (s, 2H, C_4H_2S). ^{31}P NMR spectrum (CD_3CN): δ 27.1 (s).

[{(Phtpy)(PPh$_3$)$_2$Ru}$_2$(C≡C(C$_4$H$_2$S)$_2$C≡C)](ClO$_4$)$_2$ (10). This compound was prepared by the same procedure as that of **9** except for using 5,5′-bis(trimethylsilylethynyl)-2,2′-bithiophene instead of 2,5-bis(trimethylsilylethynyl)thiophene. Yield: 74%. Anal. Calcd for $C_{126}H_{94}Cl_2N_6O_8P_4Ru_2S_2$: C, 66.34; H, 4.15; N, 3.68. Found: C, 66.58; H, 4.07; N, 3.59. ESI-MS: *m*/*z* (%) 1147 (20) $[\{(Phtpy)(PPh_3)_2Ru\ C{\equiv}C(C_4H_2S)_2C{\equiv}C\}]^+$ 1041 (100) $[M - (ClO_4)_2]^{2+}$, 673 (20) $[\{(Phtpy)(PPh_3)Ru\}]^+$. IR spectrum (KBr, cm^{-1}): ν 2040 m (C≡C), 1088 s (ClO_4). ^1H NMR spectrum (CD_3CN, ppm): δ 9.06−7.15 (m, 90H, tpy and C_6H_5), 7.03 [d, 2H, $^3J(H^4H^3)$ or $(H^{4'}H^{3'})$ = 6 Hz, $H^{4,4'}$], 6.88 [d, 2H, $^3J(H^3H^4)$ or $(H^{3'}H^{4'})$= 6 Hz, $H^{3,3'}$]. ^{31}P NMR spectrum (CD_3CN): δ 28.1 (s).

[{(Phtpy)(PPh$_3$)$_2$Ru}$_2$(C≡C(C$_4$H$_2$S)$_3$C≡C)](ClO$_4$)$_2$ (11). This compound was prepared by the same procedure as that of **9** except for using 5,5″-bis(trimethylsilylethynyl)-2,2′:5′,2″-terthiophene instead of 2,5-bis(trimethylsilylethynyl)thiophene. Yield: 77%. Anal. Calcd for $C_{130}H_{96}Cl_2N_6O_8P_4Ru_2S_3$: C, 66.07; H, 4.09; N, 3.56. Found: C, 66.12; H, 4.05; N, 3.61. ESI-MS: *m*/*z* (%) 1229 (15) $[(Phtpy)(PPh_3)_2Ru(C{\equiv}C(C_4H_2S)_3C{\equiv}C)]^+$, 1082 (100) $[M - (ClO_4)_2]^{2+}$, 673 (50) $[\{(Phtpy)(PPh_3)Ru\}]^+$. IR spectrum (KBr,

Table 3. Crystallographic Data for **2**·2H_2O·2$C_2H_4Cl_2$, **4**·Et_2O, and **6**

	2·2H_2O·2$C_2H_4Cl_2$	**4**·Et_2O	**6**
empirical formula	$C_{114}H_{96}Cl_4N_6O_4P_4Ru_2S_2$	$C_{110}H_{90}N_6O_3P_4Ru_2$	$C_{57}H_{44}N_3OP_2Ru$
temp, K	293(2)	293(2)	293(2)
space group	$P\bar{1}$	$P\bar{1}$	$P2_1/n$
a, Å	10.330(4)	11.783(2)	12.903(4)
b, Å	13.537(5)	18.919(4)	18.013(5)
c, Å	19.439(6)	22.607(5)	20.338(5)
α, deg	81.008(8)	109.165(2)	
β, deg	82.970(9)	96.648(3)	96.855(5)
γ, deg	82.577(7)	96.144(2)	
V, Å^3	2648.0(15)	4671.3(17)	4693(2)
Z	1	2	4
ρ_{calcd}, g cm^{-3}	1.346	1.329	1.344
μ, mm^{-1}	0.541	0.448	0.446
radiation (λ, Å)	0.710 73	0.710 73	0.710 73
R1(F_o)[a]	0.0671	0.0419	0.0613
wR2(F_o)[b]	0.2043	0.0863	0.1476
GOF	1.106	1.050	1.113

[a] $R1 = \Sigma|F_o - F_c|/(\Sigma F_o)$. [b] $wR2 = \Sigma[w(F_o^2 - F_c^2)^2]/\Sigma[w(F_o^2)]^{1/2}$.

cm^{-1}): ν 2040 m (C≡C), 1087s (ClO_4). ^{1}H NMR spectrum (CD_3-CN, ppm): δ 8.78−7.04 (m, 90H, tpy and C_6H_5), 6.98 (s, 2H, $H^{3'}H^{4'}$), 6.92 [d, 2H, $^3J(H^4H^3)$ or ($H^{4''}H^{3''}$)= 6 Hz, $H^{4,4''}$], 6.69 [d, 2H, $^3J(H^3H^4)$ or ($H^{3''}H^{4''}$)= 6 Hz, $H^{3,3''}$]. ^{31}P NMR spectrum (CD_3-CN): δ 28.4 (s).

[{(Phtpy)(PPh$_3$)$_2$Ru}$_2$(C≡C−C≡C(C$_4$H$_2$S)C≡C−C≡C)](ClO$_4$)$_2$ (12). This compound was prepared by the same procedure as that of **9** except for using 2,5-bis[(trimethylsilyl)-1,3-butadiylthiophene instead of 2,5-bis(trimethylsilylethynyl)thiophene. Yield: 59%. Anal. Calcd for $C_{126}H_{92}Cl_2N_6O_8P_4Ru_2S$: C, 67.35; H, 4.13; N, 3.74. Found: C, 67.22; H, 4.17; N, 3.81. ESI-MS: *m*/*z* (%) 1024 (100) [M − $(ClO_4)_2$]$^{2+}$, 673 (45) [{(Phtpy)(PPh$_3$)Ru}]$^+$. IR spectrum (KBr, cm^{-1}): ν 2137 m (C≡C), 2001 m (C≡C), 1090 s (ClO_4). ^{1}H NMR spectrum (CD_3CN, ppm): δ 9.03−7.13 (m, 90H, tpy and C_6H_5), 7.0 (s, 2H, C_4H_2S). ^{31}P NMR spectrum (CD_3CN): δ 29.3 (s).

[{(Phtpy)(PPh$_3$)$_2$Ru}$_2$(C≡C−C≡C(C$_6$H$_4$)C≡C−C≡C)](ClO$_4$)$_2$ (13). This compound was prepared by the same procedure as that of **9** except for using 1,4-bis[(trimethylsilyl)-1,3-butadiyl]-benzene instead of 2,5-bis(trimethylsilylethynyl)thiophene. Yield: 53%. Anal. Calcd for $C_{128}H_{94}Cl_2N_6O_8P_4Ru_2$: C, 68.60; H, 4.23; N, 3.75. Found: C, 69.05; H, 4.35; N, 3.79. ESI-MS: *m*/*z* (%) 1021 (100) [M − $(ClO_4)_2$]$^{2+}$, 673 (25) [{(Phtpy)(PPh$_3$)Ru}]$^+$. IR spectrum (KBr, cm^{-1}): ν 2151 m (C≡C), 2003 m (C≡C), 1089 s (ClO_4). ^{1}H NMR spectrum (CD_3CN, ppm): δ 9.04−7.15 (m, 94H, tpy, C_6H_5 and C_6H_4). ^{31}P NMR spectrum (CD_3CN): δ 29.4 (s).

[{(Phtpy)(PPh$_3$)$_2$Ru}$_2$(C≡C(C$_6$H$_4$)C≡C)](ClO$_4$)$_2$ (14). [(Phtpy)-(PPh_3)$_2$RuCl](ClO$_4$) (150 mg, 0.14 mmol) and silver perchlorate (30.0 mg, 0.14 mmol) were dissolved in acetone (50 mL). After the solution was stirred under reflux for half an hour, it was cooled to room temperature and filtered to remove the silver chloride precipitate. To the brown filtrate were added 1,4-bis(ethynyl)-benzene (10.0 mg, 0.07 mmol) and triethylamine (1 mL). The solution was then stirred under reflux for 1 day to give a red brown residue by removing the solvent in vacuo. The product was purified by chromatography on a neutral alumina column using dichloromethane−acetone (10:1) as an eluent to collect the second band. Yield: 85%. Anal. Calcd for $C_{124}H_{94}Cl_2N_6O_8P_4Ru_2$: C, 67.91; H, 4.32; N, 3.83. Found: C, 68.23; H, 4.41; N, 3.72. ESI-MS: *m*/*z* (%) 997 (60) [M − $(ClO_4)_2$]$^{2+}$, 797 (75) [{(Phtpy)(PPh_3)RuC≡C(C_6H_4)C≡C}]$^+$ 673 (100) [{(Phtpy)(PPh$_3$)Ru}]$^+$. IR spectrum (KBr, cm^{-1}): ν 2063 m (C≡C), 1091 s (ClO_4). ^{1}H NMR spectrum (CD_3CN, ppm): δ 9.17−7.15 (m, 94H, tpy, C_6H_5 and C_6H_4) ^{31}P NMR spectrum (CD_3CN): δ 29.2(s).

[{(Phtpy)(PPh$_3$)$_2$Ru}$_2$(C≡C(C$_6$H$_4$)$_2$C≡C)](ClO$_4$)$_2$ (15). This compound was prepared by the same procedure as that of **9** except for using 4,4′-bis(trimethylsilyethynyl)biphenyl instead of 2,5-bis-(trimethylsilylethynyl)thiophene. Yield: 67%. Anal. Calcd for $C_{130}H_{98}Cl_2N_6O_8P_4Ru_2$: C, 68.81; H, 4.35; N, 3.70. Found: C, 69.01; H, 4.38; N, 3.75. ESI-MS: *m*/*z* (%) 1035 (100) [M − $(ClO_4)_2$]$^{2+}$, 1135 (10) [{(Phtpy)(PPh_3)$_2$Ru}(C≡C(C_6H_4)$_2$C≡C)]$^+$, 673 (15) [{-(Phtpy)(PPh$_3$)Ru}]$^+$. IR spectrum (KBr, cm^{-1}): ν 2060 m (C≡C), 1087 s (ClO_4). ^{1}H NMR spectrum (CD_3CN, ppm): δ 9.17−7.13 (m, 98H, tpy, C_6H_5 and C_6H_4). ^{31}P NMR spectrum (CD_3CN): δ 29.2 (s).

[{(Phtpy)(PPh$_3$)$_2$Ru}$_2$(C≡CC≡CC≡CC≡C)](ClO$_4$)$_2$ (16). This compound was prepared by the same procedure as that of **9** except for using 1,4-bis(trimethylsilylethynyl)-1,8-octadiyne instead of 2,5-bis(trimethylsilylethynyl)thiophene. Yield: 52%. Anal. Calcd for $C_{122}H_{90}Cl_2N_6O_8P_4Ru_2$: C, 67.68; H, 4.19; N, 3.88. Found: C, 68.01; H, 4.25; N, 3.80. ESI-MS: *m*/*z* (%) 983 (60) [M − $(ClO_4)_2$]$^{2+}$, 1031 (10) [{(Phtpy)(PPh_3)$_2$Ru}(C≡CC≡CC≡CC≡C)]$^+$, 673 (100) [{(Phtpy)(PPh$_3$)Ru}]$^+$. IR spectrum (KBr, cm^{-1}): ν 2110 s (C≡C), 1951 s (C≡C),1086 s (ClO_4). ^{1}H NMR spectrum (CD_3CN, ppm): δ 9.03−6.93 (m, 90H, tpy and C_6H_5). ^{31}P NMR spectrum (CD_3CN): δ 29.3 (s).

Crystal Structural Determination. Crystals coated with epoxy resin or sealed in capillaries with mother liquors were measured on a Rigaku Mercury CCD diffractometer. Reflection data were collected at room temperature by the ω scan technique using graphite-monochromated Mo Kα (λ = 0.710 73 Å) radiation. An absorption correction by multiscan was applied to the intensity data. The structures were solved by direct method, and the heavy atoms were located from E-map. The remaining non-hydrogen atoms were determined from the successive difference Fourier syntheses. The non-hydrogen atoms were refined anisotropically, whereas the hydrogen atoms were generated geometrically with isotropic thermal parameters. The structures were refined on F^2 by full-matrix least-squares methods using the SHELXTL-97 program package.[57] Crystallographic data for **2**, **4**, and **6** were summarized in Table 3.

Physical Measurements. Elemental analyses were performed on a Perkin-Elmer model 240C automatic instrument. The electrospray mass spectra (ESI-MS) were recorded on a Finnigan LCQ mass spectrometer using dichloromethane−methanol as the mobile

(57) Sheldrick, G. M. *SHELXL-97, Program for the Refinement of Crystal Structures*; University of Göttingen: Göttingen, Germany, 1997.

phase. The UV−vis−NIR spectra were measured on a Perkin-Elmer Lambda 900 UV−vis−NIR spectrometer. The IR spectra were recorded on a Magna 750 FT-IR spectrophotometer using KBr pellets. The ^{1}H and ^{31}P NMR spectra were measured on a Varian UNITY-500 spectrometer with $SiMe_4$ as the internal reference and 85% H_3PO_4 as the external standard. The cyclic voltammogram (CV) and differential pulse voltammogram (DPV) were made with a potentiostat/galvanostat model 263A in dichloromethane solutions containing 0.1 M $(Bu_4N)(PF_6)$ as the supporting electrolyte. The CV was performed at a scan rate of 100 mV s^{-1}. The DPV was measured at a rate of 20 mV s^{-1} with a pulse height of 40 mV. Platinum and glassy graphite were used as the counter and working electrodes, respectively, and the potential was measured against a Ag/AgCl reference electrode. The potential measured was always referenced to the half-wave potentials of the ferrocenium/ferrocene couple ($E_{1/2} = 0$).

Acknowledgment. This work was supported financially by the NSFC (Grants E90401005, E20490210, E20521101, and E20625101), the NSF of Fujian Province (Grant E0420002), and the Key Project from CAS (Grant KJCX2-YW-H01).

Supporting Information Available: Tables giving UV−vis−NIR absorption spectral data of $Ru_2^{II,II}$, $Ru_2^{II,III}$, and $Ru_2^{III,III}$ complexes in dichloromethane, figures giving additional UV−vis−NIR spectra, cyclic and differential pulse voltammograms, magnetic susceptibility, and X-ray crystallographic file in CIF format for the structure determination of compounds **2, 4**, and **6**. This material is available free of charge via the Internet at http://pubs.acs.org.

IC700412M